GENE EXPRESSION AND BIOCHEMISTRY OF ISOPRENOID BIOSYNTHESIS IN THE GLANDULAR SECRETORY TRICHOMES OF *ARTEMISIA ANNUA*

A Thesis Submitted to the College of Graduate Studies and Research

in Partial Fulfillment of the Requirements for the Degree of

Master of Science

in the Department of Biochemistry

University of Saskatchewan

Saskatoon

By

Devin R. Polichuk

PERMISSION TO USE

In presenting this thesis in partial fulfillment for a M.Sc. degree from the University of Saskatchewan, I agree that the Libraries of this University may make it freely available for inspection. I further agree that permission for copying of this thesis in any manner, in whole or in part, for scholarly purposes maybe be granted by the Head of the Department of Biochemistry or the Dean of the College of Graduate Studies and Research. It is understood that in copying, publication, or use of this thesis or parts thereof for financial gain shall not be allowed without my written permission. It is also understood that due recognition shall be given to me and to the University of Saskatchewan in any scholarly use which may be made of any materials in my thesis.

Requests for permission to copy or to make other use of material in this thesis in whole or in part should be addressed to:

Head of the Department of Biochemistry

University of Saskatchewan

Saskatoon, Saskatchewan

S7N 5E5

Canada

ABSTRACT

The Chinese herb *Artemisia annua* possesses small 10-cell biseriate glandular trichomes on the surface of its aerial tissues. These trichomes were isolated from floral tissue using a Bead Beater based method. Expression patterns of expressed sequence tags from a trichome library whose Basic Local Alignment Search Tool (BLAST) results suggested a possible function in terpenoid metabolism were investigated by RT-PCR. Known terpenoid biosynthetic enzymes, such as amorpha-4,11-diene synthase showed a high degree of trichome-specific expression. In order to investigate cell specific gene expression within the trichome, the promoter for the gene encoding amorpha-4,11-diene synthase was isolated but the lack of an efficient transformation protocol in *A. annua* hindered reporter gene localization experiments. Traditional and whole-mount *in situ* hybridization techniques were used to further the study of cell specific gene expression within the glandular trichome. An RNA probe constructed from the sequence of amorpha-4,11-diene synthase localized expression to the 2nd and 3rd subapical cell pairs of the glandular trichomes. This suggests that at least part of the artemisinin biosynthetic pathway resides within the lower cell pairs. To better understand the genes involved in terpenoid biosynthesis in *A. annua*, the full length sequence of a short chain alcohol dehydrogenase highly represented in an expressed sequence tag library and shown to have trichome-specific expression by RT-PCR, was cloned. Heterologous expression in *Escherichia coli* demonstrated that the enzyme was capable of oxidizing a wide range of monoterpenols to their corresponding ketone forms. All of this data helps us to better understand the organization of expression and biochemistry of terpenoids in *A. annua* glandular trichomes.

ACKNOWLEDGEMENTS

I would like to take this opportunity to thank the people who have supported me during my Master's studies. I would like to thank my supervisor, Dr. Patrick Covello, for giving me this wonderful opportunity to work on such a novel project in his lab. I am thankful for his generosity, understanding and financial support that he provided during my studies. I would also like to acknowledge Darwin Reed without whom I would not have been able to learn as much as I have during my time here. I must also thank Dr. Thomas Teoh and Dr. Yansheng Zhang who provided me with excellent company and guidance throughout my project. As well, Drs. Rong Li and Dauenpen Meesapyodsuk were good colleagues, always willing to give advice and a kind word. I also thank Goska Nowak, Shawn Gibson, Sarah Steinback, Melanie Dauk, and many others at PBI for acting as sounding boards whenever I wanted to release my frustrations and needed a good ear.

I would like to thank Drs. Khandelwal, Georges, Warrington, and Wang for being on my committee.

Foremost, I would like to thank Dr. Prapapan Teerawanichpan who was the reason I made it to the end.

My greatest appreciation goes to my family: to my father who taught me the value of working hard and with honour; to my mother who taught me to never let go of a goal and to persevere in the face of adversity; and to my brothers who support me in all my endeavours.

TABLE OF CONTENTS

LIST OF TABLES

LIST OF FIGURES

LIST OF ABBREVIATIONS

AaMTADH	Artemisia annua Monoterpene Alcohol Dehydrogenase
AMDS	Amorpha-4,11-diene synthase
BLAST	Basic Local Alignment Search Tool
bp	Base Pairs
DB	Debris
DMAPP	Dimethylallyl Pyrophosphate
EGTA	Ethylene glycol-bis(2-aminoethyl ether) N,N,N', N'-tetra-acetic acid
FDS	Farnesyl Diphosphate Synthase
FPP	Farnesyl Pyrophosphate
GC	Gas Chromatography
GPP	Geranyl Pyrophosphate
GST	Glandular Secretory Trichome
GSTSUB	Glandular Secretory Trichome Minus Flower Bud
IPP	Isopentenyl Pyrophosphate
ISH	*In situ* Hybridization
MDR	Medium Chain Reductase
MS	Mass Spectrometry
NGT	Nonglandular Trichome
PCR	Polymerase Chain Reaction
P450	Cytochrome P450
RS	Restriction Site
RT	Reverse Transcriptase/Transcription
RT-PCR	Reverse Transcriptase – Polymerase Chain Reaction

SDR	Short Chain Alcohol Dehydrogenase/Reductase
SDW	Sterile Distilled Water
WISH	Whole-mount *In situ* Hybridization

1. INTRODUCTION

Isoprenoids are an incredibly diverse and ubiquitous natural product group that is found in all plant species. They are the oldest class of biomolecules with evidence of their existence extending 2.5 billion years ago (Lange *et al.*, 2000). Numbering over 30,000 identified compounds, they are involved in electron transport chains, membrane composition, hormones, photosynthetic pigments, and plant defense compounds. In industry, monoterpenes are commonly used as fragrant additives to cosmetics and food. Sesquiterpenes, such as the sesquiterpene lactones found in the Anthemideae tribe of Asteraceae are known for their medicinal value. The foremost being artemisinin from the annual herb *Artemisia annua*. It is because of this compound that studies on *A. annua* terpenoid biosynthesis have exploded in the past 2 decades. This has resulted in *A. annua* becoming the model plant for biseriate trichome biology at this point in time.

Previous studies (Duke *et al.*, 1994; Duke and Paul, 1993), have implicated the biseriate glandular trichomes present on the leaves, stems, and flowers of *A. annua* as the biosynthetic site for mono and sesquiterpenes. These studies provided circumstantial evidence in the form of ultrastructural studies of the trichomes showing the production of exudates in the gland cells. As well, a glandless biotype was isolated which showed no detectable accumulation of artemisinin. However, no direct evidence for the expression of genes involved in terpenoid biosynthesis in the trichomes has been presented.

This thesis describes a study undertaken to investigate the genes involved in terpenoid biosynthesis in the glandular trichomes of *A. annua*. Analysis of the localization of terpenoid biosynthesis within the trichome, isolation of trichome specific promoters, and identification of genes involved in terpenoid biosynthetic pathways will allow for the development of tools to further the terpenoid engineering research currently underway worldwide.

2. LITERATURE REVIEW

2.1. Asteraceae

Asteraceae is one of the highly medicinal families consisting of a wide range of plants that has colonized almost all the continents of the world. It possesses 11 subfamilies: the most well known being Chicorioideae and Asteroideae. These subfamilies can be further divided into tribes. Asteroideae, for example, possesses 21 tribes. The members of Asteraceae are usually recognized by having composite flowers (Schutz *et al.*, 2006). Asteraceae are herbs (Absinthe wormwood, tarragon, Jerusalem artichoke), shrubs (lettuce, chicory, marigolds) and less commonly trees (tree daisy, tree marigold). Some members are economically important as vegetables, such as lettuce (*Lactuca sativa*) and chicory (*Chicorium intybus*). Some are a common sight in floral gardens; marigolds (*Chrysanthemum x morifolium*) and daisies (*Bellis perennis)*. Some members are recognized as important weeds, including dandelion (*Taraxacum officinale*) and ragwort (*Senecio jacobaea*). In the past couple of decades, *A. annua*, a member of the Anthemideae tribe of the Asteroideae has become one of the most popular medicinal plants in the world. *A. annua* is a Chinese herb commonly referred to as annual wormwood, sweet Annie, or Qing hao (green herbs) (Ferreira *et al.*, 1997). However, recent reports have suggested that Qing hao has been erroneously associated with *A. annua* and that the true ancient chinese name is huang hua hao (Hsu, 2006).

2.2. A. annua

2.2.1. Horticulture

A. annua is an herb whose history originates in China. It has now been introduced and grown in many countries around the world including Argentina, Bulgaria, France, Hungary, Romania, Italy, Spain, the United States, and the former Yugoslavia (Klayman, 1989; Klayman, 1993). Considered to be a weed, *A. annua* is a vigorous plant that can grow in a wide range of conditions but is best suited to the moist conditions of the Chinese forests. This highly aromatic, single-stemmed plant can grow to around 2 meters tall and possesses many 2.5-5.0 centimeter long, deeply dissected leaves on alternating branches (Figure 2.1) (Hall, 1932). *A. annua* is an annual plant which sets it apart from most of the other 400 members of

the Artemisia genus which are mostly biennial or perennial and is the reasoning behind its species name. The plant grows vegetatively during days longer than 14 hours (Ferreira *et al.*, 1995). Days of less than 14 hours induce the reproductive growth of *A. annua*. Within 3 weeks small flowers appear throughout the plant. The highly aromatic florets are arranged into very small 1-3 millimeter capitula usually appearing greenish or yellowish. This aromatic nature has made *A. annua* useful for the construction of wreaths, flavourings and essential oil. Somewhat unique for *Artemisia* species, *A. annua* seems to be reliant on insects and wind for pollination (McVaugh, 1984).

Figure 2.1. Photographs of *A. annua* foliage (left) and developing floral buds (right).

2.2.2. Historical Importance

A. annua's pharmacological use began in ancient Chinese medicine (Ferreira *et al.*, 1997; Hsu, 2006). One of the first recorded uses of *A. annua* can be found in the *Chinese Handbook of Prescriptions for Emergency Treatments* of 340 AD where it is recommended for the treatment of fevers. In 1527, a Chinese herbalist, Li Shi-Zhen, recommended *A. annua* for the treatment of childhood fevers and a closely related plant *Artemisia apiacea* for the treatment of the then unknown disease we know today as malaria. In 1971, Chinese researchers isolated a cold diethyl ether extract that showed anti-malarial activity. The active component in the extract, artemisinin, was purified and in 1972 the unusual structure was defined (Klayman, 1985). It is a sesquiterpene lactone that possesses an endoperoxide bridge. It was found to be extractable from all aerial tissues of the plant, with very high content in the

capitula, but not in pollen grains or root tissue. Roots transformed with *Agrobacterium rhizogenes* have also been reported to produce artemisinin (Banerjee *et al.*, 1997; Weathers *et al.*, 2004). Modern investigations into the activity of artemisinin have shown it to have possible uses in cancer therapy (Efferth, 2006; Nakase *et al.*, 2007; Withers and Keasling, 2007), tryptanosomiasis (Kaiser *et al.*, 2002; Stephenson and Wiselka, 2000), hepatitis (Paeshuyse *et al.*, 2006; Romero *et al.*, 2005), and as a herbicide (Lee, 2007).

2.3. Trichomes

2.3.1. Structure and Function of Trichomes

Trichomes are specialized hairs that have evolved for a variety of functions. In the model plant Arabidopsis, they are found on the aerial surfaces of the plant but are not found on roots, hypocotyls, cotyledons, petals, stamens, and carpels (Marks, 1997). Trichome development and morphogenesis have been extensively studied in Arabidopsis mutants (Marks, 1997). Trichomes are developed on the leaf surface at an early stage of leaf development when the developing epidermis (protoderm) is still dividing rapidly. Trichome development starts from specification of trichome cell, cell enlargement, elongation of the cell perpendicular to the plane of the leaves, and ends in branching (Hulskamp *et al.*, 1994; Schwab *et al.*, 2000).

Trichomes are derived from epidermal cells and perform a wide range of functions. Some secrete sticky exudates to trap insects; others produce essential oil to attract beneficial insects or repel pests (Levin, 1973; Wang *et al.*, 2001a). Non-biosynthetic roles, in which no exudates is produced, for trichomes also exist as their physical presence can deter insects trying to reach the epidermis (Levin, 1973; Schoonhoven *et al.*, 2005). Their presence can also modulate air flow over the leaf surface affecting respiration and transpiration rates. Photodamage can be prevented as well through blockage of some of the light reaching on the surface of the leaf (Johnson, 1975). In addition to the physical functions, trichomes possess a chemical defense function as they accumulates a vast array of bioactive chemicals in many plants (Bhakuni *et al.*, 2001; Iijima *et al.*, 2004; Turner and Croteau, 2004; Venkatachalam *et*

al., 1984; Yamaura *et al.*, 1992). The 3 common types of glandular trichomes in plants are capitate (*Nicotiana tabacum*), peltate (*M. piperita*), and biseriate (*A. annua*). Capitate trichomes have elongated stalks with a globular head. Peltate trichomes have short stalks with a flattened disc-shaped head. Biseriate trichomes are comprised of 2 vertical columns of cells from the base to the tip of the trichome.

2.3.2. Trichome Investigations in *A. annua*

The structure and development of trichomes on leaves and floral buds of *A. annua* was analyzed extensively by light and electron microscopy (Duke and Paul, 1993; Ferreira and Janick, 1995). *Artemisia* species possess two types of trichomes (Figure 2.2)(Ferreira and Janick, 1995) The large 5-cell T-shaped filamentous trichome, which does not produce essential oil, is very abundant on leaf, stem, and bract tissues but completely absent from the florets. It is possible that this trichome functions in a similar manner to the nonglandular trichomes of Arabidopisis. The 10-cell biseriate glandular trichome is found sparsely throughout the aerial tissues of the plant where it is indented in the epidermis (Figure 2.3). The glandular trichomes are densely packed and exposed around the florets of the capitula (Figure 2.4A). The cuticle surrounding the apex of the biseriate trichome detaches and forms a sac-like reservoir for essential oil excreted by the apical cells. The trichomes on the florets have been shown previously to rupture and senesce after anthesis which would presumably release attractants for insect pollinators. It is at this point that artemisinin content in the plant is at its highest as well (Ferreira *et al.*, 1995). This would further implicate the trichomes in the biosynthesis and storage of artemisinin and presumably all terpenoids held within the cuticular sac. This hypothesis was further supported by the study of the glandless mutant (Duke *et al.*, 1994). This mutant was completely devoid of glandular trichomes (Figure 2.4B) and had no detectable levels of artemisinin anywhere in the plant.

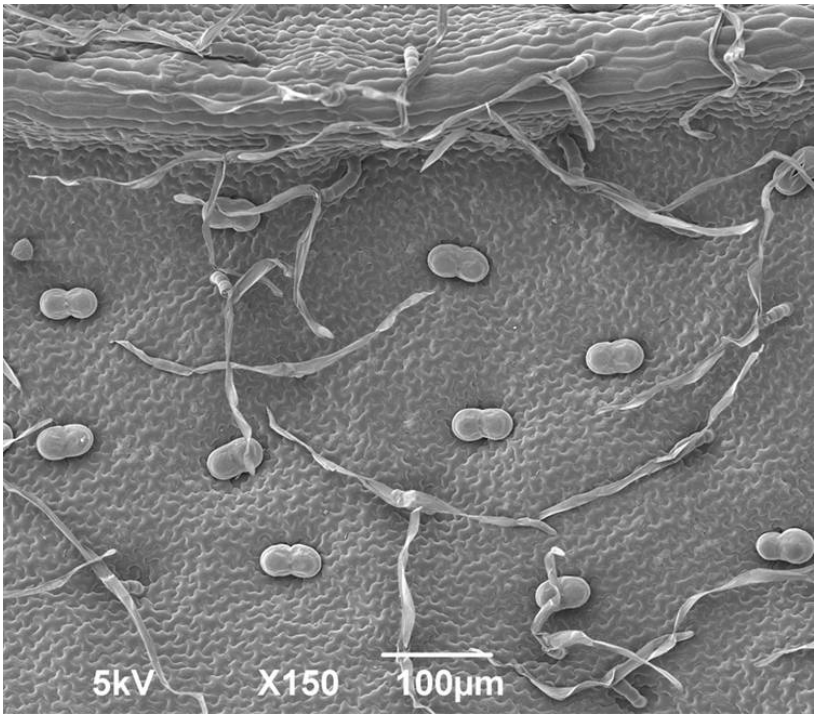

Figure 2.2. Scanning electron micrograph of an *A. annua* leaf showing both glandular and nonglandular trichomes taken from (http://www.york.ac.uk/org/cnap/artemisiaproject/index.htm).

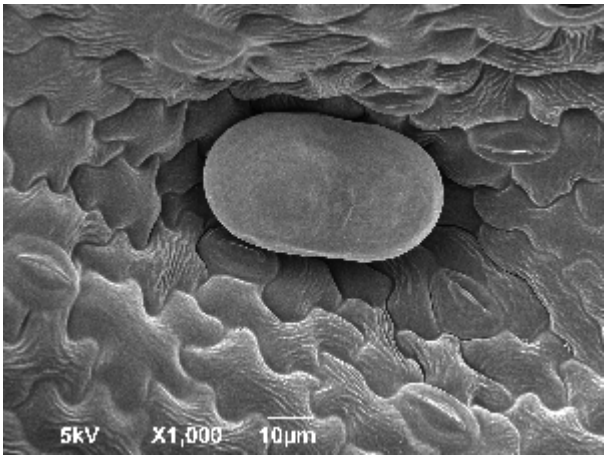

Figure 2.3. Scanning electron micrograph of an *A. annua* glandular trichome present on a leaf (http://www.york.ac.uk/org/cnap/artemisiaproject/index.htm).

A)

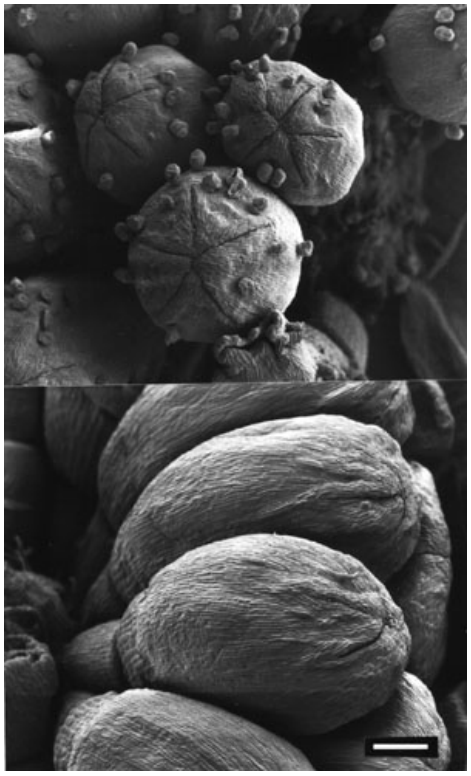

B)

Figure 2.4. Scanning electron micrograph of *A. annua* florets in A) normal and B) glandless biotypes. Reproduced with permission (Ferreira, 1996).

2.3.3. Comparison to Other Trichome Systems

Glandular trichome analyses have also been done in a member of Lamiaceae using peppermint. Peppermint (*M. piperita*) is a hybrid mint between watermint (*Mentha aquatica*) and spearmint (*Mentha spicata*). The glandular trichomes of spearmint and peppermint are morphologically different from those of the Asteraceae (Maffei and Sacco, 1987; Turner *et al.*, 2000a, b). They are peltate trichomes consisting of a disc-shaped arrangement of cells held up on a single stalk cell. They produce exclusively monoterpenes and have a wide range of use in culinary and essential oil products (McKay and Blumberg, 2006). In order to investigate the metabolism of the trichomes, a bead abrasion method was developed for the isolation of the secretory cell disc from mint trichomes (Gershenzon *et al.*, 1992). This method was also applied to other plants, most notably Tansy which is a relative of *A. annua* and possesses similar trichome architecture. A cDNA library constructed from the isolated mint trichomes was enriched in terpenoid biosynthetic genes and illustrated the importance of

isolating the trichomes to determine the biosynthetic pathways of chemicals held therein (Croteau *et al.*, 2005; Lange *et al.*, 2000). Various other trichome isolation methods had been also developed for other trichomes including the capitate trichomes of *Nicotiana* spp. and *Cannabis* spp. Most of these involve the use of liquid nitrogen, dry ice or EGTA to increase the brittleness of the base of the stalk cell and a light abrasion with a brush to dislodge the trichomes (Sirikantaramas *et al.*, 2005; Yerger *et al.*, 1992; Zhang and Oppenheimer, 2004). The simplest method, the epidermal peel, relies on having a robust leaf structure which is not found in *Artemisia* spp. (Croteau, 1977; Lessire *et al.*, 1982) One method that had proved relatively successful on *Artemisia tridentata* involved a fairly rough procedure of blending floral buds in a Waring blender followed by discontinuous Percoll gradient centrifugation to separate the resultant mixture (Slone and Kelsey, 1985).

The main difference between the trichomes of the *A. annua* and the trichomes of mint and tobacco is that in *A. annua* the trichomes have a high degree of cellular organization. There are 5 cell pairs, all of which seem to be fairly distinct from each other upon TEM analysis (Duke and Paul, 1993). It is impossible to determine visually exactly which cell pairs contribute to terpenoid biosynthesis in *A. annua*. *A. annua* trichomes possess a nongreen apical cell pair, 2 pair of green cells, and finally another 2 pairs of nongreen cell pairs. This cellular organization is vastly different from that of the capitate and peltate trichomes. The "head" on a "stalk" structure of capitate/peltate trichomes and the presence of exudate around the head of those trichomes have led many researchers to conclude that the biosynthetic cells were in fact the cells composing the head of the trichome (Wagner, 1991). However, *A. annua* has no such structure and the trichome looks very similar from the apex to the bottom upon light inspection. Supporting evidence for this model came with the visualization of lipophilic substances accumulating within those cells (Dell, 1978; Fahn, 1988) . Confirmation of this model was achieved by localization of *M. piperita* monoterpene biosynthetic enzymes to the secretory disc of the peltate trichome (Turner and Croteau, 2004). In mint trichomes, all of the secretory cells of the disc appear to be equivalent. Therefore, fragmentation of the disc, apart from cell death, should not result in the lower representation of biosynthetic pathways. In *A. annua*, lipophilic material was observed in the apical 3 cell pairs (Duke and Paul, 1993). If the same logic applies as in the other trichome systems, this suggests again

that the trichome and not the epidermis is the biosynthetic tissue for the terpenoids seen in the essential oil. Furthermore, if one wishes to analyze the gene expression of an *A. annua* trichome, one will need to isolate the top 3 or 4 cell pairs to achieve an accurate representation of the trichome's biosynthetic machinery.

2.4. Terpenoids

2.4.1. Terpenoid Structure and Biosynthesis

Terpenoids (also referred to as isoprenoids) are one of the largest groups of the natural products, universally found in all living organisms (Sacchettini and Poulter, 1997). Terpenoids play an important role in physiological functions, such as pathogen defense (saponins, artemisinin, phytoalexins) and mutualistic interactions (pheromones) (Gershenzon and Dudareva, 2007). Some take the form of hormones such as cytokinins, gibberellins and abscisic acids in plants and progestogens, androgens in animals (Dewick, 2002). Others are useful in other aspects such as cholesterol, vitamin A and D, and carotenoids. Plant terpenoids are extensively used for their aromatic and biochemical properties (Harrewijn *et al.*, 2001). They have been used as anti-microbial, anti-cancer and in other pharmaceutical applications (Harrewijn *et al.*, 2001; Rohmer, 1998; Swanson and Hohl, 2006). They have also been used in agricultural and cosmetic industries (Harrewijn *et al.*, 2001). The structure of terpenoids is highly variable, but is basically derived from a definite number of 5 carbon isoprene units (2-methylbuta-1,3-diene) (Harrewijn *et al.*, 2001).

There are at least two pathways for terpenoids biosynthesis; the mevalonate and non-mevalonate pathways. Mevalonic acid pathway is the classical pathway, which was discovered in 1950s (Figure 2.5) (Bach, 1995; Bloch, 1992). This pathway is active in the cytosol and found in all higher eukaryotes and many bacteria. The non-mevalonate pathway is also known as MEP/DOXP pathway (2-C-methyl-D-erythritol 4-phosphate/1-deoxy-D-xylulose 5-phosphate) (Figure 2.5). This pathway was recently discovered (Eisenreich *et al.*, 1998; Hunter, 2007; Rohmer, 1998) and it is present in the plastids of plants and green algae as well as in apicomplexan protozoa (Eisenreich *et al.*, 1998). Both routes, fundamentally,

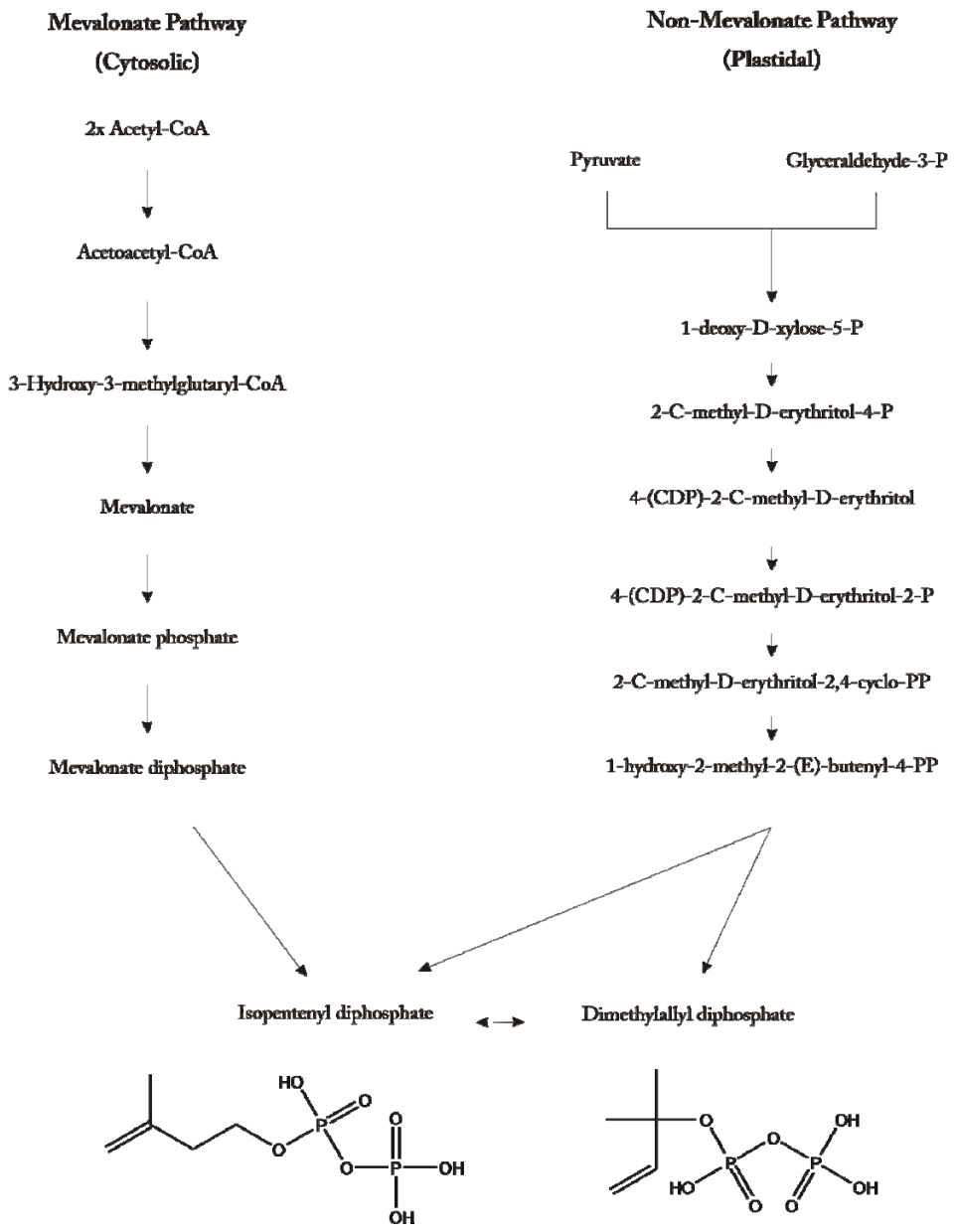

Figure 2.5. Mevalonate and Non-Mevalonate pathways for isoprenoid biosynthesis (Dubey *et al.*, 2003).

generate isopentenyl diphosphate (IPP) and dimethylallyl diphosphate (DMAPP), which are hemiterpenes (C5). The condensation of IPP and DMAPP via the enzyme geranyl pyrophosphate synthase yields geranyl pyrophosphate (GPP), which serves as a precursor for

most terpenoid biosynthesis. In order to make the larger terpenoids (sesqui, di, tri), other synthases are required which add the requisite amount of IPP units. More recently, the enzymes in monoterpene biosynthesis in peppermint trichomes were shown to localize in different cell compartments, including endoplasmic reticulum, cytosol, plastid and mitochondrion. This suggests the intracellular mobilization between different cell compartments of monoterpene intermediates (Turner and Croteau, 2004).

2.4.2. Composition of *A. annua* Essential Oil

In the Asteraceae family, it is known that glandular trichomes located on the aerial tissues of the plants are responsible for the storage of the terpenoid compounds produced by the plant. This family produces 2 main types of terpenoids which accumulate in the trichome: Aromatic volatile monoterpenes and nonvolatile sesquiterpenes. The composition of essential oil of *A. annua* was determined among different genotypes (Bhakuni *et al.*, 2001; Ferreira *et al.*, 1997). Although the relative amount of each constituent tends to vary among different genotypes, the same chemicals are present throughout (Bhakuni *et al.*, 2001). Abundant monoterpenes found in the oil include camphor, borneol, pinocarveol, artemisia ketone, artemisia alcohol, and 1,8-cineole. Abundant sesquiterpenes include germacrene D, delta-cadinene, and artemisinic acid/dihydroartemisinic acid (possible artemisinin precursors). Artemisinin is the most important chemical in the aspect of medicinal applications, however, it is present in *A. annua* at a very low level (0.01-0.8% dry weight) (Bhakuni *et al.*, 2001; Ferreira *et al.*, 1997). The common monoterpenes, including camphor, are used as an insect repellent, cough suppressant, and even in the synthesis of carbon nanotubes (Kumar and Ando, 2006).

2.5. Artemisinin

2.5.1. Known Enzymes in the Artemisinin Biosynthesis Pathway

Artemisinin is a sesquiterpene found in *A. annua*, *A. apiacea*, and *Artemisia lancea* (Hsu, 2006). Its carbon skeleton is derived from farnesyl pyrophosphate, a common precursor in the plant cell, which is formed by the condensation of 3 isoprene units. Although the structure was solved in 1979 (Liu *et al.*, 1979), the gene responsible for the first committed

step in the pathway, amorpha-4,11-diene synthase, was not isolated until 1999 (Bouwmeester *et al.*, 1999). The second enzyme in the pathway responsible for the important oxidation of amopha-4,11-diene to artemisinic alcohol was recently isolated and characterized (Teoh *et al.*, 2006). The p450 hydroxylase, CYP71AV1, was also shown to be able to further oxidize artemisinic alcohol to artemisinic acid. There are still enzymes in the pathway that are left to be characterized. The proposed pathway is show in Figure 2.6 (Teoh *et al.*, 2006). The pathway is based on the recent biochemical work done using semisynthetic intermediates fed to crude lysates of trichome, leaf, and flower (Bertea *et al.*, 2005). However, there has been research indicating that artemisinic acid is the precursor to artemisinin (Li *et al.*, 2006). This idea has been strongly refuted by research to the contrary (Brown and Sy, 2004; Brown and Sy, 2007; Sy and Brown, 2002).

2.5.2. Biotechnological Production of Artemisinin

Due to relatively low level of artemisinin in *A. annua* (0.01-0.8 %) (Bhakuni *et al.*, 2001; Ferreira *et al.*, 1997), several strategies have been adopted to increase artemisinin production to meet the demand in the medical market. This includes plant tissue culture, chemical synthesis, biotransformation and genetic engineering of *A. annua* (Abdin *et al.*, 2003). The artemisinin content in plant is influenced by several factors, such as light, water, temperature, nutrition, and biotic stresses (Ferreira *et al.*, 2005). *In vitro* plant tissue culture is, therefore, an alternative way to maintain a stable artemisinin content in the plants. Tissue culture of shoots, calli suspension culture, and hairy roots have been investigated (He *et al.*, 1983; Liu *et al.*, 2004; Liu *et al.*, 1997; Nair *et al.*, 1986; Weathers *et al.*, 1994; Woerdenbag *et al.*, 1993). Attempts to increase artemisinin production by adjusting the nutrients, hormones, growth condition, elicitors, and stresses were also reported (Liu, 2003; Qian *et al.*, 2007; Wang and Tan, 2002; Wang *et al.*, 2001b). However, the artemisinin content from tissue cultures is inconsistent and non-reproducible in some cases (Jaziri *et al.*, 1995; Tawfig *et al.*, 1989). Chemical synthesis of artemisinin is possible but complicated and not feasible for large scale production due to the complex structure of artemisinin (Jefford, 2007; Jung *et al.*, 2004; O'Neill, 2005). Heterologous expression of artemisinin metabolic pathway in microorganisms, such as *Escherichia coli* and *Saccaromyces cerevisiae* is an attractive way

due to the low cost carbon source and feasibility of large scale preparation (Chang and Keasling, 2006; Ro *et al.*, 2006). Genetic engineering of *A. annua* has become attractive since

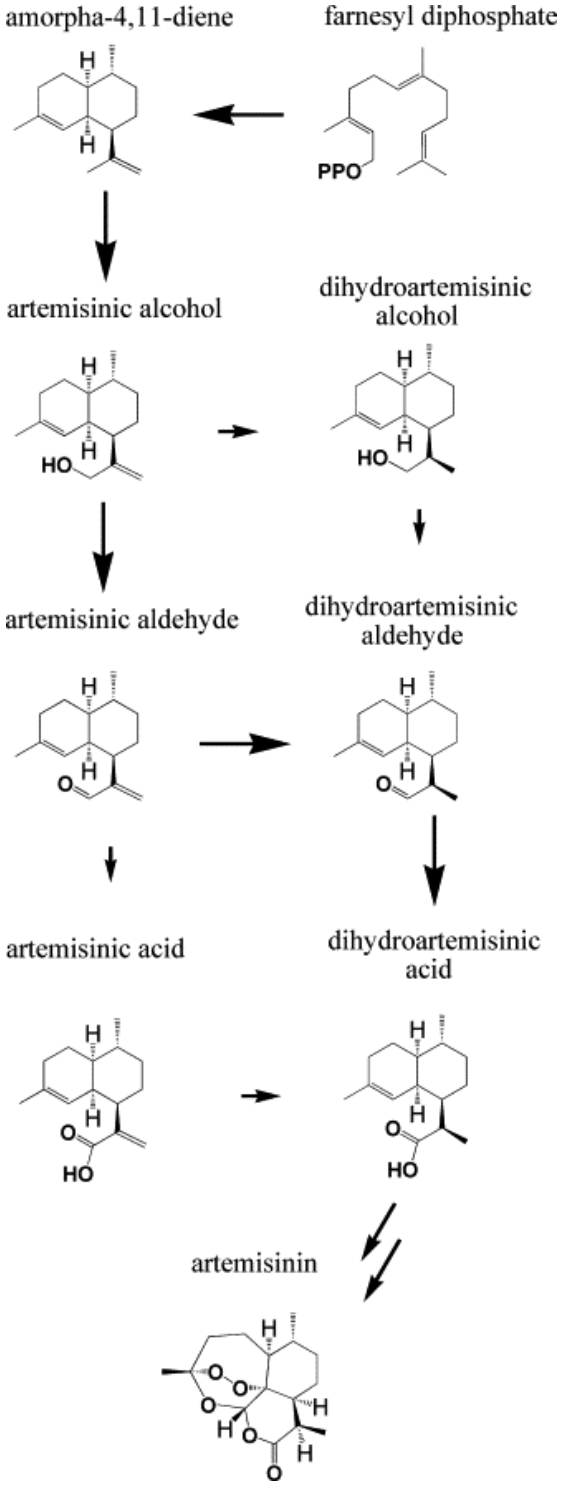

Figure 2.6. Proposed pathway for the biosynthesis of artemisinin in *A. annua*. Reproduced with permission (Teoh *et al.*, 2006).

the transformation of *A. annua* was established (Banerjee *et al.*, 1997; Ghosh *et al.*, 1997; Han *et al.*, 2005; Vergauwe *et al.*, 1997). Modulation of terpenoid biosynthesis either by over-expressing the rate-limiting enzymes or by suppressing enzymes in other pathways that compete for its precursor would allow the enhancement of artemisinin content. Over-expression of cotton farnesyl diphosphate synthase (FDS) in *A. annua* was shown to increase the artemisinin content 2-4 fold (Chen *et al.*, 1999; Chen *et al.*, 2000).

2.6. Monoterpenes

Monoterpenes are highly abundant and volatile compounds found in the essential oil of many plants. There are 3 main classes of monoterpenes which are determined by their physical structure. These are acyclic (eg. ocimene), monocyclic (eg. limonene) and bicyclic (e.g. α-pinene) (Figure 2.7)(Loza-Tavera, 1999).

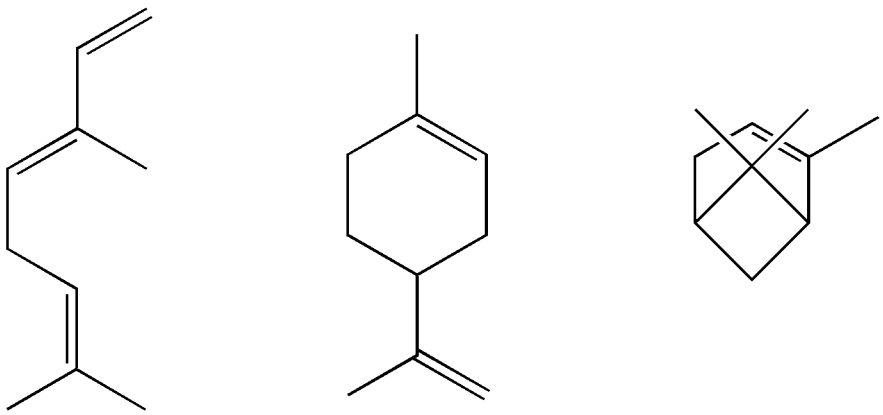

Figure 2.7. Structures representative of the 3 classes of monoterpenes: acyclic, monocyclic, and bicyclic.

Regardless of their structure they all are derived from the same C10 precursor, geranyl diphosphate. The vast array of different carbon skeleton structures comes from the monoterpene cyclase enzymes. Oxygen-containing functional groups (alcohols, aldehydes/ketones) are common occurrences and initially arise from 2 sources. In the case of borneol, it comes from the hydrolysis of the diphosphate group from bornyl pyrophosphate

(Croteau and Karp, 1979). In the case of carveol, the alcohol group is formed through the involvement of the P450 enzyme, limonene 6'- hydroxylase (Lupien *et al.*, 1995). Further oxidations/reductions by dehydrogenases/double-bond reductases also occur and depend on the individual monoterpene in question. The full proposed biosynthetic pathway for camphor is shown in Figure 2.8 (Croteau *et al.*, 1981).

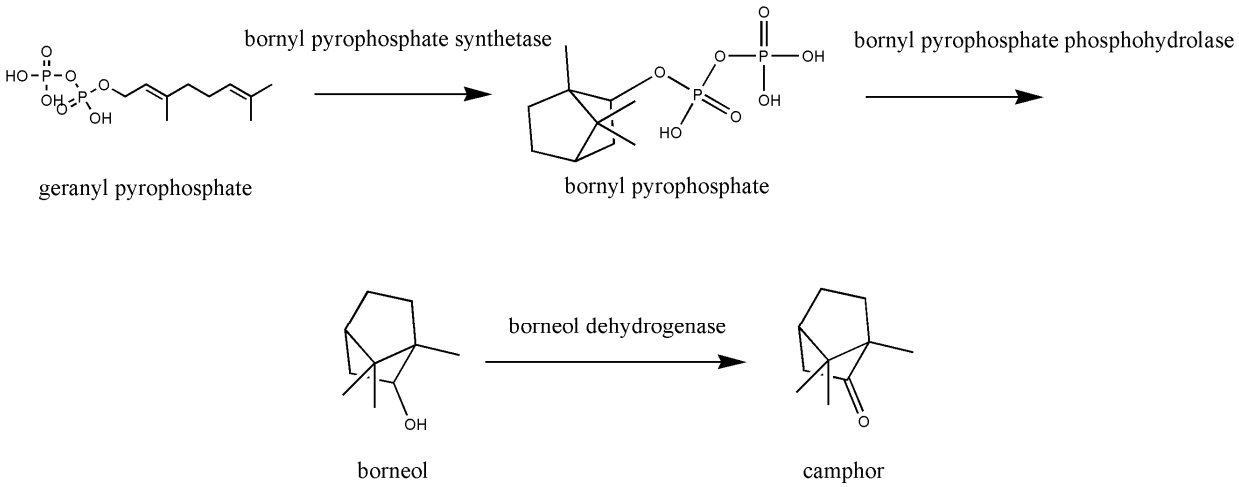

Figure 2.8. Proposed biosynthetic pathway for camphor in *Salvia officinalis*.

A smaller class of irregular monoterpenes also exists. This group has a different biosynthetic origin than regular monoterpenes. Instead of the head to tail condensation of an IPP unit to a DMAPP unit, there is a head to head condensation of two DMAPP units (Umlauf *et al.*, 2004). The removal of the pyrophosphate group proceeds in a manner different than found in the camphor example previously described. Instead there appears to be a quenching of a carbocation intermediate by a hydroxide ion. The prominent irregular monoterpene in *A. annua* is artemisia ketone (Charles *et al.*, 1991; Teixeira da Silva, 2004). Through the feeding of ^{13}C-glucose the proposed biosynthetic pathway for artemisia ketone was supported for *Tanacetum vulgare* L (Figure 2.9) (Seigler, 1995; Umlauf *et al.*, 2004).

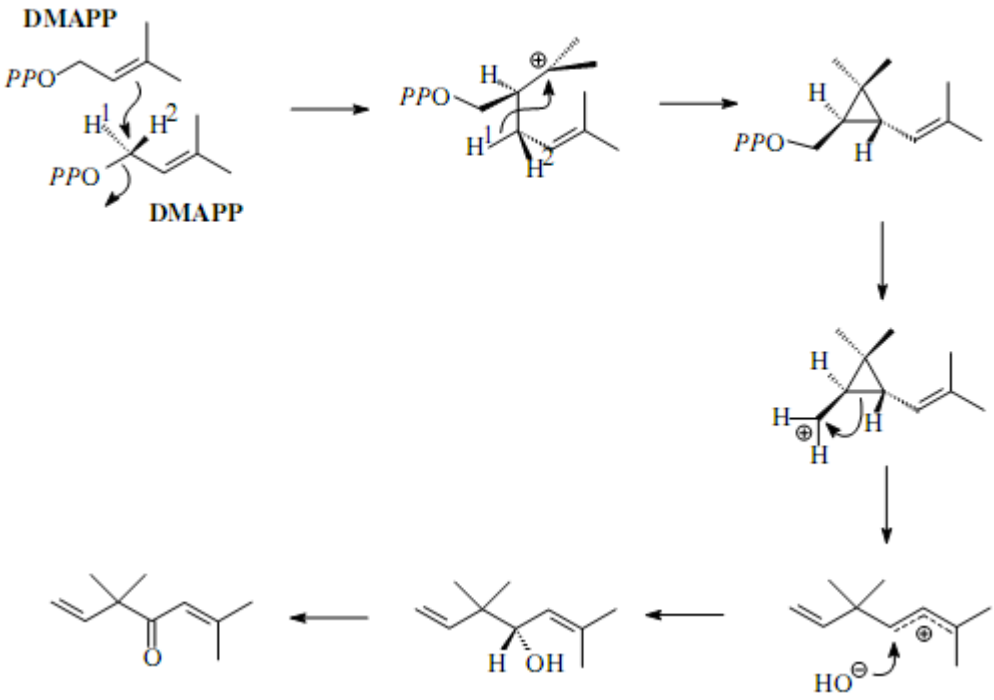

Figure 2.9. Proposed biosynthetic pathway for artemisia ketone. Reproduced with permission (Seigler, 1995; Umlauf *et al.*, 2004).

Although monoterpenes are abundant in nature, the essential oils of the plants that produce them can be very economically important. In the US alone, mint oil and related products are worth at least $5.5 billion (Lange and Croteau, 1999). Although the essential oil of *A. annua* gains it primary value from the antimalarial sesquiterpene artemisinin, one could use the information gained from studying its monoterpene biosynthetic machinery to better engineer the essential oil of a different species (Lange and Croteau, 1999). Furthermore, apart from their fragrant nature, some monoterpenes have roles in modulating insect interaction and could be produced in a plant that is requiring protection or attraction of some insect (Wagner *et al.*, 2004).

3. RATIONALE AND OBJECTIVES

3.1. Experimental Rationale

Research into the production of terpenoid compounds in the Anthemideae tribe of Asteraceae remains sparse. The enzymes and site(s) involved in the biosynthesis of the compounds such as camphor or artemisinin within *A. annua* is largely unknown. These compounds are easily extracted from the foliage of the plant which possesses secretory glandular trichomes. It is probable that these structures are responsible for the biosynthesis of terpenoid compounds in *A. annua*. Therefore, analyzing the gene expression and localization of terpenoid biosynthetic genes within these trichomes should provide insight into the production, transport and storage of terpenoid compounds in *A. annua* and related species.

3.2. Specific Aims

- **#1: Development of a method for the isolation of glandular trichomes from *A. annua.***
- **#2: Gene expression analysis of genes with a putative function in isoprenoid metabolism in *A. annua.***
- **#3: Cellular localization of isoprenoid metabolism in *A. annua*.**
- **#4: Characterization of *A. annua* monoterpene alcohol dehydrogenase.**

4. MATERIALS AND METHODS

4.1. Reagents and Distributors

The following tables detail the reagents used in this study. The distributors of the reagents used and their addresses are listed. Tables detailing the oligonucleotides and the solutions used in this research are also included.

Table 4.1. Reagents and Materials

Reagent	Distributor Name
18S rRNA universal primers	Ambion
5-bromo-4-chloro-3-indolyl-beta-D-galactopyranoside (X-gal)	Sigma-Aldrich
20:20:20 (N:P:K) plant fertilizer	Plant Products Inc.
Agarose	Invitrogen
Alkaline phosphatase conjugated anti-digoxigenin fabs (sheep)	Roche Applied Science
Ammonium acetate	Sigma-Aldrich
Ampicillin	Sigma-Aldrich
Artemisia ketone	Sigma-Aldrich
Bovine serum albumin fraction V (BSA)	Sigma-Aldrich
Bromophenol Blue	Sigma-Aldrich
Chloramphenicol	Sigma-Aldrich
Deoxynucleotide triphosphates (NTPs)	Invitrogen
Dichloromethane	Fisher Scientific
DNase I	GE Healthcare
Ethanol (95%)	Fisher Scientific
Ethylene-diamine-tetraacetic acid (EDTA)	Fisher Scientific
Ethylene-glycol-tetraacetic acid (EGTA)	Sigma-Aldrich
Formalin	Stratagene
Formamide	Roche Applied Science
Glacial acetic acid	Fisher Scientific
Glass beads	Biospec Products Inc.
Glycerol	Sigma-Aldrich
Helium	Prax-air
Heparin	Sigma-Aldrich
HEPES	Sigma-Aldrich

Heptane	Fisher Scientific
HISTRAP columns (1mL)	GE Healthcare
HPLC-grade water	Sigma-Aldrich
Imidazole	GE Healthcare
Isopropanol	Sigma-Aldrich
Isopropyl β-D-1-thiogalactopyranoside (IPTG)	Sigma-Aldrich
Kanamycin	Sigma-Aldrich
Levamisole	Sigma-Aldrich
Luria broth base	Sigma-Aldrich
Magnesium chloride	Sigma-Aldrich
Magnesium sulfate	Sigma-Aldrich
β-mercaptoethanol	Sigma-Aldrich
Methanol	Fisher Scientific
Methyl cellulose	Sigma-Aldrich
MOPSO	Sigma-Aldrich
β-Nicotinamide adenine dinucleotide (NAD+)	Sigma-Aldrich
β-Nicotinamide adenine dinucleotide phosphate (NADP+)	Sigma-Aldrich
Nitro blue tetrazolium chloride/ 5-Bromo-4-chloro-3-indolyl phosphate (NBT/BCIP)	Roche Applied Science
Nylon mesh	Smallparts Inc.
Paraplast chips	Fisher Scientific
PD-10 desalting columns	GE Healthcare
(-)-*trans*-pinocarveol	Sigma-Aldrich
Polyvinylpyrrolidone (MW ~40,000)	Sigma-Aldrich
Potassium chloride	Sigma-Aldrich
Potassium phosphate, monobasic	Sigma-Aldrich
Potassium phosphate, dibasic	Sigma-Aldrich
Powerscript II Reverse Transcriptase	Invitrogen
Precast acrylamide gels	Bio-Rad
Probe-on Plus microscope slides	Fisher Scientific
Proteinase K	Invitrogen
Protein assay dye reagent concentrate	Bio-Rad
Restriction Endonucleases	New England Biolabs
Ribonucleotides	Stratagene
RNase A	Sigma-Aldrich
RNase Out	Invitrogen
Sodium acetate	Sigma-Aldrich
Sodium borohydride	Sigma-Aldrich

Sodium chloride	Sigma-Aldrich
Sodium phosphate, dibasic	Sigma-Aldrich
Sodium phosphate, monobasic	Sigma-Aldrich
Sorbitol	Sigma-Aldrich
SP6 RNA Polymerase	Stratagene
Sprint Advantage PCR tubes	BD Biosciences
Sucrose	Sigma-Aldrich
T3 RNA Polymerase	Fisher Scientific
T4 DNA ligase	New England Biolabs
T7 RNA Polymerase	Fisher Scientific
Taq DNA Polymerase	Invitrogen
Thiourea	Sigma-Aldrich
Tris-HCl	Sigma-Aldrich
Trizol reagent	Invitrogen
Tween-20	Sigma-Aldrich
Vent DNA Polymerase	New England Biolabs
XAD-4 Resin	Sigma-Aldrich
Xylene	Sigma-Aldrich
Xylene cyanol	Sigma-Aldrich
Yeast tRNA	Sigma-Aldrich

Table 4.2. Names and Addresses of Distributors

Supplier	**Address**
Agilent Technologies	Agilent Technologies, Santa Clara, California, USA
Ambion	Ambion Inc., Austin, Texas, USA
BD Biosciences	BD Biosciences, Mississauga, Ontario, Canada
Bio-Rad	Bio-Rad Laboratories, Mississauga, Ontario, Canada
Biospec Products Inc.	Biospec Products Inc. http://www.biospec.com
Dutch Growers	Dutch Growers, Saskatoon, Saskatchewan, Canada
Elixir Farm Botanicals	Elixir Farm Botanicals, Brixey, Missouri, USA
Fisher Scientific	Fisher Scientific, Winnipeg, Manitoba, Canada
GE Healthcare	GE Healthcare Bio-Sciences Inc., Baie D'Urfe, Quebec, Canada
Invitrogen	Invitrogen Canada Inc. Burlington, Ontario
New England Biolabs	New England Biolabs Inc., Pickering, Ontario, Canada

Plant Products Inc.	Plant Products Inc., Brampton, Ontario, Canada
QIAGEN	QIAGEN Inc., Missisauga, Ontario, Canada
Roche Applied Science	Roche Diagnostics Canada, Laval, Quebec, Canada
Sigma-Aldrich	Sigma-Aldrich, Oakville, Ontario, Canada
Smallparts Inc.	Smallparts Inc., Miramar, Florida, USA
Stratagene	Stratagene, La Jolla, California, USA

Table 4.3. List of Solutions

Abbreviation	**Buffer or Solution**	**Components**
TIB1	Trichome Isolation Buffer 1	25 mM HEPES pH 7.3, 200 mM sorbitol, 10 mM sucrose, 5 mM dithiothreitol, 10 mM KCl, 5 mM $MgCl_2$, and 0.5 mM potassium phosphate, pH 7.3
TIB2	Trichome Isolation Buffer 2	25 mM MOPSO pH 6.3, 200 mM sorbitol, 10 mM sucrose, 5 mM thiourea, 2 mM dithiothreitol, 5 mM $MgCl_2$, 0.5 mM sodium phosphate, pH 6.3, and 1% (w/v) PVP (MW 40,000) ; [0.6% methyl cellulose]
FAA	FAA	50 % ethanol, 5 % acetic acid, 10 % formalin
FB	Fixation Buffer	PBS containing 0.1% Tween-20, 0.08 M ethylene glycol-bis(2-aminoethyl ether) N,N,N', N'-tetra-acetic acid (EGTA), 5% formaldehyde
PBT	PBT	PBS containing 0.1% Tween-20
HS	Hybridization Solution	50% formamide, 5X SSC (pH 7.0), 50 µg/mL heparin
NTE	NTE	500 mM NaCl, 10 mM Tris-HCl, pH 7.5, 1 mM ethylenediaminetetra-acetic acid (EDTA)
BS	Blocking Solution	2% bovine serum albumin fraction V, 0.1% Tween-20 in PBT
SB	Staining Buffer	100 mM NaCl, 50 mM $MgCl_2$, 100 mM Tris-HCl, pH 9.5, 0.1% Tween-20

SSB	Staining Stop Buffer	PBT with 20 mM EDTA
	DNA Extraction Buffer	100 mM Tris-HCl, pH 7.5, 500 mM NaCl, 50 mM EDTA, 10mM β-mercaptoethanol, 1% SDS (v/v)
	Binding Buffer	20 mM sodium phosphate pH 7.4, 500 mM NaCl, 50 mM imidazole, 10 mM β-mercaptoethanol, 10% glycerol
	Elution Buffer	20 mM sodium phosphate pH 7.4, 500 mM NaCl, 300 mM imidazole

Table 4.4. List of Oligonucleotides

Name	**Primer Sequence**	**Annealing Temp Used (^{o}C)**
AABIGU	5'-AATGAGGAGTATGCCCAAACC-3'	54
AABIGL	5'-GGAAATTCGTGCGATATGTGTAGT-3'	54
RS-1BAM	5'-TAATACGACTCACTATAGGGNNNNNNNNNNGGATCC-3'	54
RS-2ECO	5'-TAATACGACTCACTATAGGGNNNNNNNNNNGAATTC-3'	54
RS-3HIND	5'-TAATACGACTCACTATAGGGNNNNNNNNNNAAGCTT-3'	54
RS-4XBA	5'-TAATACGACTCACTATAGGGNNNNNNNNNNTCTAGA-3'	54
PRAMS1	5'-CTATCTGTTCCACCCCTTGCTCT-3'	54
PRAMS2	5'-GCAATGGGGCGAATAGGTTT-3'	54

M13UP	5’-TGTAAAACGACGGCCAGT-3’	Sequencing
M13RP	5’-CAGGAAACAGCTATGAC-3’	Sequencing
AMDSRTU	5’-CGGCGCAGTACATTCCTTTCTA-3’	54
AMDSRTL	5’-GTCCCTCATTTGCCCATTTTG-3’	54
CYP71AV1RTU	5’-GGACGATTTCGGAACTCATAA-3’	54
CYP71AV1RTL	5’-CTCCTCTGGTAAAGCGCGTGTAG-3’	54
MTADHRTU	5’-ATCGGAGAATGTATTGTGAGGTTA-3’	54
MTADHRTL	5’-ATATCTTGTGGTCCGAGTGTCTTC-3’	54
ADHNDEU	5’-CATATGGCTTCTTTAACTCCAAAAGC-3’	54
ADHBAML	5’-GGATCCTTACGGTTTCCATGAAAATAAACC-3’	54
ALDH1RTU	5’-GGCCAAAGGAAGAAAGGAAGACA-3’	54
ALDH1RTL	5’-TAATCACGCCATCAGGAACACCAG-3’	54
DBR1RTU	5'-TCTTTTACTCCTGGTTCGCCTCTA-3'	54
DBR1RTL	5'-TCCTCCAACGTTCTCAAAGTAAAT-3'	54

4.2. Trichome Isolation

4.2.1. Growth of *M. piperita* and *A. annua*

M. piperita (variety chocolate mint) plants (Dutch Growers) were grown on a laboratory bench top (September to November) and watered as required.

A. annua seed (Elixir Farm Botanicals) was germinated in a photoperiod of 16 h and temperature regiment of 25^{o}C/20^{o}C. The plants were watered as required with a dilute solution of 20:20:20 (N:P:K) (Plant Products Inc.) fertilizer. As growth required, the plants were transplanted from starter pots to 6 inch pots and finally to 12 inch pots. Flowering of *A. annua* was induced by transferring the plants, as needed, to a photoperiod of 12 h and temperature regiment of 25^{o}C/20^{o}C for 18-22 d.

4.2.2. Trichome Isolation from *Mentha* x *piperita*

Trichome isolation was performed as previously described with minor modifications (Gershenzon *et al.*, 1992). *M. piperita* leaves were imbibed with ice cold distilled water for 1 h and subsequently placed in a 350 mL Bead Beater (Biospec Products Inc.). One hundred grams of 500 μm diameter glass beads (Biospec Products Inc.) and 1 g/g leaf tissue of XAD-4 resin (Sigma-Aldrich) was also added. The Bead Beater chamber was then topped up with TIB1 buffer (Table 4.2). The leaves were abraded on ice for 4 x 1 min intervals at 75-90 V controlled by a rheostat (Staco Energy Products, 3PN1010). The chamber was allowed to cool down for 1 minute between intervals.

The resulting homogenate was then filtered through 350 μm, 105 μm, and finally 20 μm nylon mesh (Smallparts Inc). The material retained on the 20 μm mesh was collected and analyzed under a light microscope.

4.2.3. Trichome Isolation from *A. annua*

Initial trichome isolation experiments were performed as described above. *A. annua* leaves, from vegetatively growing plants, were isolated from the top one third of mature plants. They were then abraded in the Bead Beater in the same manner as the *M. piperita* leaves. Abrasion voltages of 48 - 110 V were tested.

Subsequent experiments utilized a newer protocol with minor modifications (Lange *et al.*, 2000). Leaves were imbibed in distilled water and abraded in a similar manner; however, using TIB2 buffer. The beads were changed to 100 μm glass beads. In later experiments leaves were replaced by floral buds. Abrasion voltages of 48 - 110 V were tested. As well 0.6% w/v methyl cellulose was added to the TIB2 buffer. The 105 μm nylon mesh was replaced by 90 μm mesh. Eventually only 500 μm glass beads were used. A further optimized abrasion interval was later determined by Dr. Thomas Teoh.

4.3. Gene Expression Analysis

4.3.1. Isolation of RNA from *A. annua*

Root tissue was harvested from mature plants and thoroughly washed to remove soil particles. It was then frozen in liquid N_2 and stored at -80^{o}C until use. Root RNA was isolated using RNeasy RNA Isolation Kit (QIAGEN) according to manufacturer's instructions.

Leaf tissue was harvested from the top one-third of mature plants and frozen in liquid N_2 until needed. Floral tissue was harvested from plants that had been transferred to 12 h daylight conditions for 20 d. The buds were frozen in liquid N_2 and stored until required. Both leaf and floral RNA were isolated using Trizol Reagent (Invitrogen) according to manufacturer's instructions.

Trichomes were harvested as described earlier and the RNA was isolated either by using RNeasy RNA Isolation Kit (QIAGEN) according to manufacturer's instructions with the addition of an initial 1 min 0.5 s intermittent sonication, or by Dr. Thomas Teoh for cDNA library construction as previously described (Logemann *et al.*, 1987).

4.3.2. Reverse Transcription-Polymerase Chain Reaction Analysis

Prior to the RT reaction, 200 ng of each RNA was treated with 1 U of FPLC-pure DNase I (GE Healthcare) and 40 U of RNase OUT (Invitrogen) in the presence of 1X first-strand buffer (Invitrogen) at 37^{o}C for 15 min. Reverse transcription was carried out using Superscript II (Invitrogen) according to manufacturer's instructions with random hexamers (Invitrogen). Subsequently, 1 μL of the RT reaction was added to the corresponding PCR amplification. Advantage 2 polymerase mix (BD Biosciences) was used for the PCR reactions according to manufacturer's instructions. Oligonucleotide primers AMDSRTU and AMDSRTL (Table 4.3) were used to monitor expression of amorpha-4,11-diene synthase (AMDS)(AAF98444). CYP71AV1RTU and CYP71AV1RTU were used for expression analysis of CYP71AV1 also known as amorpha-4,11-diene hydroxylase (ABC41927).

MTADHRTU and MTADHRTL were used to look at expression of *A. annua* monoterpene alcohol dehydrogenase (AaMTADH). ALDH1RTU and ALDH1RTL were used to analyse gene expression of *A. annua* aldehyde dehydrogenase 1 (AaALDH1). Finally, DBR1RTU and DBR1RTL were use to analyse expression of *A. annua* double bond reductase 1(AaDBR1). Amplicons were cloned into pCRII-TOPO and at least 10 independent clones were sequenced to confirm primer specificity.

Universal 18S rRNA primers (Ambion) were used according to manufacturer's instructions as an internal normalization control.

4.4. Cell-Specific Gene Expression Analysis

4.4.1. *In Situ* Hybridization (ISH)

In situ hybridization was carried out as previously described with minor modifications (Cox *et al.*, 1988). Floral tissue was fixed in FAA for 3 h with occasional shaking. Samples were held at a vacuum pressure of 500 mmHg 3 times for 5 min during the incubation using an *Arabidopsis* transformation chamber. Samples were then dehydrated in a series of ethanol (in water) solutions 2 x 50 % and 1x 60 %, 70 %, 80 %, 95 % (v/v)(30 min each) and left overnight in 100 % ethanol at room temperature. The samples were then cleared with 25 %, 50 %, 75 % (30 min each), and 2 x 100 % (1 h) of xylene (in ethanol). Paraplast chips (Fisher Scientific) were added to the 100 % xylene and the samples were incubated at 42^{o}C overnight. Afterwards, more chips were added and the samples were incubated for another 4h. This was repeated twice. The xylene/paraplast solution was then replaced with fresh molten paraplast prepared in a 60^{o}C incubator. The sample was incubated at 60^{o}C and the paraplast solution was changed every 8-12 h for 4-6 d.

Wax blocks were made by placing the samples in fresh paraplast solution and orienting the buds in glycerol lubricated molds using a gradient heatblock. The molds were then placed on the top of ice slurry. Once completely hardened, they were submerged in the slurry overnight. The embedded samples were then removed from the molds and stored at 4^{o}C.

For sectioning, individual flower buds were cut out of the mold and mounted for use in a microtome. Sections 5 μm – 10 μm thick were cut using a Leica RM2165 microtome, and subsequently mounted on Fisher Probe-On Plus slides (Fisher Scientific). Sections were analyzed by light microscopy for the presence of sectioned trichomes.

4.4.2. Whole Mount *In situ* Hybridization (WISH)

Whole mount *in situ* hybridization was performed as previously described with minor modifications (Engler *et al.*, 1998).

4.4.2.1. Prehybridization Treatments

Trichomes, isolated as described earlier, were incubated in a 1:1 solution of fixation buffer and heptane for 20-45 min with vigorous shaking to ensure emulsion of the heptane. Samples were then dehydrated 2 x 5 min in methanol and 3 x 5 min in ethanol. Samples were then stored at -20^{o}C in either ethanol if they were going to be processed within 3 d or in 70% ethanol if they were to be stored for a longer time.

Samples were removed from -20^{o}C storage and rinsed once in ethanol. They were then incubated in a 1:1 mixture of ethanol/xylene for 30 min. Then the samples were washed 2 x in ethanol and 2 x in methanol. Subsequently, they were washed in a 1:1 methanol:PBT mixture. Samples were postfixed in PBT containing 5% formaldehyde for 30 min. They were then digested for 10-45 min in PBT containing 40 μg/mL of proteinase K at room temperature. Digestion was halted by washing the samples in PBT containing 0.2% glycine for 5 min. Samples were rinsed 2 x with PBT and postfixed in PBT containing 5% formaldehyde for 30 min. They were then rinsed 3 x in PBT and equilibrated in a 1:1 PBT:HS solution for 5 min. Samples were rinsed 2 x in HS and prehybridized in HS for 1-2 h at 50-55^{o}C.

4.4.2.2. Probe Construction

A probe for amorpha-4,11-diene synthase was amplified from genomic DNA using the oligonucleotides AABIGU and AABIGL to generate a 591 base pair amplicon which was then cloned into pCR2.1-TOPO (Invitrogen) and subsequently subcloned using *Eco*RI into pBLUESCRIPT KS- (Stratagene). Two μg of the plasmid was then digested with either *Hind*III (antisense) or *Bam*HI (sense) for 2 h. *Bam*HI digested plasmid was transcribed using either T7 or T3 polymerase (Stratagene) and 10 μM of each ribonucleotide (uridine triphosphate, 6.5 μM:3.5 μM unlabelled:digoxygenin labeled) (Roche) for 2.5 h at 37^{o}C. 10 units of DNase I (GE Healthcare) was added and incubated for 1 h to remove the plasmid template. The RNA was then precipitated with ammonium acetate/ethanol. The pellet was then resuspended in carbonate buffer and incubated at 65^{o}C for the calculated amount of time to yield theoretical 150 base pair fragments. The following equation was used (Long, J, http://carnegiedpb.stanford.edu/research/barton/in_situ_protocol.html):

Time=Li-Lf/(K•Li•Lf)

Li=initial length of probe (in kb)

Lf=final length of probe (0.15 kb)

K=0.11 $kb^{-1}min^{-1}$

The solution was then neutralized with the addition of 100 μl 10% acetic acid and precipitated using ammonium acetate/ethanol. RNA was resuspended in 30 μL of DEPC-treated water and its concentration was determined spectrophotometrically. The RNA was then diluted to a concentration of 1 μg/μL. In subsequent unsuccessful experiments pCRII-TOPO (Invitrogen) replaced pCR2.1-TOPO and pBLUESCRIPT KS-, data not shown.

4.4.2.3. Hybridization

Samples were transferred to 1.5 mL Eppendorf tubes with 600 µL HS. DIG-labelled RNA probe at a final concentration of 3 µg/mL and yeast tRNA (Sigma-Aldrich) at a final concentration of 100 µg/mL were added to the sample after being denatured at 85°C for 5 min. Hybridization was done at 50-55°C overnight with mild continuous shaking.

4.4.2.4. Post Hybridization

Samples were washed 2 x 30 min at 50-55°C in HS. They were then incubated for 15 min in a 1:1 solution of HS:NTE. The samples were rinsed 2 x with NTE and then incubated with NTE containing 40 µg/mL RNaseA (Sigma-Aldrich) at 37°C for 45 min. Samples were transferred to glass tubes and washed 3-5 x with NTE at room temperature for 15 min. Subsequently, they were incubated in 1:1 mixture of NTE:PBT for 5 min. They were then rinsed with PBT and incubated with BS for 30-120 min.

4.4.2.5. Antibody Incubation and Chromogenic Reaction

Fresh BS, containing 1:1500 diluted alkaline phosphatase conjugated anti-digoxigenin fab fragments (Roche), was incubated at 4°C overnight with inversion. Samples were incubated for 10 min with BS and then washed 4 x 30 min with PBT. Samples were then equilibrated in SB 2 x 5 min. Three milliliters of fresh SB containing 1 mM of levamisole (Sigma-Aldrich) with 60 µl of NBT/BCIP solution (Roche) were added and the samples were incubated in the dark with inversion for 24-72 h. Samples were then rinsed 2 x with SSB. To visualize any signal, samples were put on a glass slide and analyzed under a light microscope.

4.5. Amorpha-4,11-diene Promoter Isolation

4.5.1. Isolation of Genomic DNA

Genomic DNA was isolated from *A. annua* leaf tissue using a method previously described (Li and Chory, 1998). Leaf tissue was ground in a mortar and pestle with liquid N_2 and placed in a 40 mL Oak Ridge tube. Five milliliters of preheated (65^{o}C) DNA extraction buffer was added to the powdered tissue and vigorously shaken. The sample was then incubated for 10 min at 65^{o}C with occasional shaking. Subsequently, 1.67 mL of 5 M potassium acetate was added and vigorously mixed. The sample was incubated on ice for 20 min, then centrifuged in a Sorvall centrifuge at 25000 xg for 20 min. The supernatant was transferred to a new 40 mL Oak-Ridge tube and 3.33 mL of isopropanol was added and the sample was placed at -20^{o}C for 30 min. DNA was pelleted at 20000 xg for 15 min. The pellet was dried and resuspended in sterile distilled water (SDW) and transferred to a microfuge tube. The sample was extracted with phenol:chloroform (1:1) and the aqueous layer was transferred to a new tube and extracted again with chloroform. DNA was pelleted with sodium acetate/isopropanol, resuspended with SDW and the purity/yield was determined spectrophotometrically.

4.5.2. Restriction Site Polymerase Chain Reaction

Restriction site (RS) primers were designed by Dr. Janet Taylor in accordance with the guidelines outlined previously (Sarker *et al.*, 1993). Five hundred nanograms of genomic DNA was used in the PCR with 20 pmols of each RS Primer and 6.7 pmols of amorpha-4,11-diene synthase specific primers. The first PCR reaction contained prAMS1 and one of the RS primers (1-4), in separate reactions. One microliter of these reactions was then reamplified using the same RS primers and prAMS2. The conditions were as follows: 95^{o}C 10 min (before *Taq* addition, only used for primary PCR), 95^{o}C 5 min; 95^{o}C 30 s, 54^{o}C 2 min, 68^{o}C 5 min x 30 cycles; 68^{o}C 10 min. The second reaction was performed using BD Advantage Sprint tubes (BD Biosciences).

4.6. *A. annua* Monoterpene Alcohol Dehydrogenase

4.6.1. Construction of AaMTADH Expression Vector

Clone GST21F10 was isolated from a glandular trichome cDNA library created by Thomas Teoh (Teoh *et al.*, 2006). Oligonucleotide primers ADHNDEU and ADHBAML were used to amplify the full length sequence. The product was cloned into pCRII-TOPO (Invitrogen). The gene was then subcloned into pET15b using *Nde*I, *Bam*HI and T4 DNA ligase (New England Biolabs). The construct, designated pDP001, was then used to transform the *E. coli* strain BL21DE3 pLYS.

4.6.2. Expression and Purification of HIS-tagged AaMTADH

A starter culture of 10 mL for pET15b and pDP001 was grown at 37°C in LB broth with 100 mg/mL ampicillin overnight. Five milliliters of the starter culture were then added to 2 cultures of 50 mL LB broth with 100 μg/mL ampicillin which was grown at 37°C until an OD_{600} of 0.600 was reached. Then IPTG was added to a final concentration of 0.4 mM and the culture was grown at 30°C overnight. One milliliter of uninduced pET15b, induced pET15b, uninduced pDP001 and induced pDP001 were aliquoted, boiled and subjected to electrophoresis in a 4-15% Tris-HCl polyacrylamide gel (Bio-Rad) and to check for expression. The culture was centrifuged at 4°C and 5000 x *g*. The pellet was resuspended in 3 mL of binding buffer and lysed by passage through a French press 3 times. The cleared lysate was loaded on a HISTrap FF Crude column (GE Healthcare), which had been equilibrated with binding buffer (minus β-mercaptoethanol), using a peristaltic pump at ~1 mL/min flow rate. The column was washed with 15 volumes of binding buffer. Then the column was eluted with elution buffer containing 300 mM imidazole. Fractions were collected at 1 min intervals. Fractions 2-5 were pooled and loaded on a PD-10 Desalting Column (GE Healthcare) following manufacturer's instructions and the protein was eluted using 100 mM CHES, pH 9.5, with 10% glycerol.

Protein concentration was measured using the Bio-Rad Protein Assay (Bio-Rad) according to manufacturer's instructions. The r^2 value of the BSA standard curve was 0.979. The concentration of the protein was found to be 184 ng/μL. The protein was run on a 4-15%

Tris-HCl polyacrylamide gel (Bio-Rad) and stained with Brilliant Blue Protein Stain (Bio-Rad) to assess purity.

4.6.3. Enzyme Assays of AaMTADH Activity

AaMTADH enzyme assays contained 1.8 μg of purified AaMTADH HIS-tagged protein in a 100 μL assay consisting of 100 mM CHES pH 9.5 containing 10% glycerol, 1 mM DTT, 2 mM NAD+, and 65 μM substrate (Ringer *et al.*, 2005). The reactions were carried out at 30^{o}C with 400 rpm intermittent shaking for 1-1.5 hrs and were stopped and extracted with 100 μL ethyl acetate and analyzed with GC-MS. Assays for pH optimum determination contained 400 μM artemisia alcohol to ensure substrate saturation. The reactions were performed in triplicate using an incubation time of 5 min. Bicine buffer was used for pH 8.0, 8.5, and 9.0. CHES buffer was used for pH 9.0, 9.5, 10.0. CAPS buffer was used for pH 10.0, 10.5, 11.0. Artemisia ketone and (-)-trans-pinocarveol were obtained from Sigma Aldrich. Fenchol, myrtanol, thujyl alcohol, sabinyl acetate, cis-pinocarveol, borneol and piperitol were obtained from previously isolated samples from various sources in Dr. Covello's lab storage collection. Artemisinic alcohol, aldehyde and acid were obtained from Darwin Reed (Teoh *et al.*, 2006).

4.6.4. Synthesis of Artemisia Alcohol

Four hundred microliters of artemisia ketone (Sigma-Aldrich), dissolved in 10 mL of methanol, was combined with 0.4 g of sodium borohydride and reacted for 72 h at room temperature. The reaction was then quenched with the addition of water (Davidson *et al.*, 2004). Diethyl ether was used to extract the artemisia alcohol. $MgSO_4$ was added to absorb any water that had carried over. The solution was then filtered through a fiberglass filter to remove particulates. The ether was evaporated under a nitrogen flow. Ethanol was used to dissolve the artemisia alcohol. The purity of the artemisia alcohol was then assessed using GC-MS.

4.6.5. Synthesis of Sabinol

Sabinyl acetate was first saponified with 10% KOH in methanol:water (9:1) at 65^{o}C for 3 h. A volume of water was added and the solution was extracted with diethyl ether. The diethyl ether was evaporated under a nitrogen flow (Reed *et al.*, 2003). Ethanol was used to resuspend the sabinol and the purity was assessed using GC-MS.

4.6.6. Gas Chromatography/Mass Spectrometry Analysis

GC Methods named EZ70 and EZ125 were used to analyze monoterpene and sesquiterpene reactions respectively, as follows. GC/MS analysis was accomplished using an Agilent 5973 Mass Selective Detector coupled to an Agilent 6890N Gas Chromatograph using G1701DA MSD Chemstation Software (for instrument control and data analysis) and equipped with a 30M X 0.25 mm DB-5MS column with 0.25 μm film thickness (Agilent Technologies). The chromatograph conditions were a split injection (20:1) onto the column using a helium flow of 0.4 ml / min and temperature programmed with either an initial temperature of 70 °C for 1 min then temperature ramped at 10°C / min to 300°C and held at 300 °C for 10 min (EZ70) or an initial temperature of 125 °C for 1 min then temperature ramped at 5°C / min to 300°C and held for 10 minutes at 300 °C (EZ125). The mass selective detector was run under standard EI^{+} conditions scanning an effective mass range of 40 to 700 at 2.26 scan/sec.

4.6.7. Gas Chromatography Analysis

The method Chiral 70 was used to analyze both R and S isomers of the racemic mixture of the synthesized artemisia alcohol, as follows. GC analysis was accomplished using flame ionization detector coupled to an Agilent 6890 Gas Chromatograph equipped with a 30M X 0.25 mm CycloSilB column with 0.25 μm film thickness (Agilent

Technologies). The chromatograph conditions were a split injection (50:1) onto the column with a helium flow of 1 ml / min and initial temperature of 70 °C for 1 min then temperature ramped at 5°C / min to 230°C and held for 10 minutes. Data was recorded and analyzed using Agilent ChemStation software.

5. RESULTS

5.1. Trichome Isolation

5.1.1. *M. piperita*

As a prelude to *A. annua* trichome isolation, an effort was made to reproduce the results obtained with the Bead Beater protocol (Gershenzon *et al.*, 1992) by isolating the peltate trichomes from a Mint species. *M. piperita* leaf tissue provided a decent yield of secretory cell clusters using the recommended voltage. *M. piperita* trichomes are inherently different from those found in *Artemisia* species. The Bead Beater method is very well suited to flat disc shaped trichomes found on *M. piperita* leaves. The beads are able to access the trichomes easily since they lay flat and have no vertical cell stacking (Figure 5.1). Lower voltages (and hence, lower velocities) yielded a lower percentage of mesophyll and cell debris; albeit with a lowered abundance of secretory cell clusters as well (data not shown).

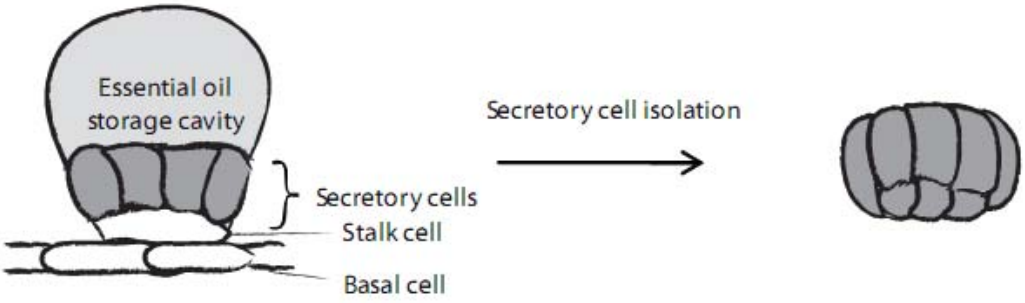

Figure 5.1. Schematic diagram showing the dislocation of the secretory disc from the peltate trichomes of *M. piperita* through the use of the Bead Beater system. Redrawn with permission (Gershenzon *et al.*, 1992).

5.1.2. *A. annua*

The trichomes of *A. annua* seemed to be amenable to this protocol as they too were protruding from the leaf surface. Therefore, it was postulated that this technique, with minor modifications, would allow us to isolate similar secretory cell clusters from the biseriate

trichomes *A. annua* (Gershenzon *et al.*, 1992). Thus, *A. annua* leaves were then subjected to the Bead Beater protocol. The isolated cells are shown in Figure 5.2A and a fully intact trichome from a flower bud preparation is shown in Figure 5.2B as a reference. The resultant preparation appeared to consist primarily of apical cells with the attached cuticular sac. This degree of trichome fragmentation was considered to be unacceptable for use in a library construction as other studies have shown that there are osmiophilic substances found in the 3 apical cell pairs which indicate their possible involvement in essential oil biosynthesis. Therefore, to ensure that we indeed had the cells responsible for terpenoid biosynthesis, we required a more intact trichome structure. The first step taken was to alter the voltage of the rheostat controlling the Bead Beater as it was possible that we were smashing the trichomes into the individual cell pairs. However, this action did not result in any difference in the ratio of apical cells to partially intact trichomes.

Further investigations lead to the observation that the leaf trichomes were slightly embedded into the leaf surface and hence the glass beads used would have a low probability of contacting the trichome's base. The abundance of apical cell pairs was hypothesized to occur as a result of the beads skipping along the surface of the leaf and hitting the top 1 or 2 protruding cell pairs, resulting in the lack of intact trichomes witnessed in the trichome preparations. With this hypothesis in mind, we proceeded to test the ability of smaller beads to isolate the trichomes. Beads with a diameter of one hundred micrometers were selected which represented a 5 x reduction of bead size. These modifications slightly increased the ratio of larger secretory cell clusters to apical cells (data not shown); however, the quality of the preparation was still not appropriate for our purposes.

Our microscopic observations, as well as previous studies (Duke and Paul, 1993; Ferreira and Janick, 1995; Slone and Kelsey, 1985), showed that trichomes on the flowers might be more accessible. These trichomes were not embedded into the surface of the florets and receptacle. As well, since these trichomes were just newly formed and they had a measured peak in artemisinin accumulation (Ferreira *et al.*, 1997), they presented a very nice opportunity to isolate trichomes that are known to be in the process of accumulating essential oil. The trichomes of the expanded leaves were already mature and it was uncertain as to

(A)

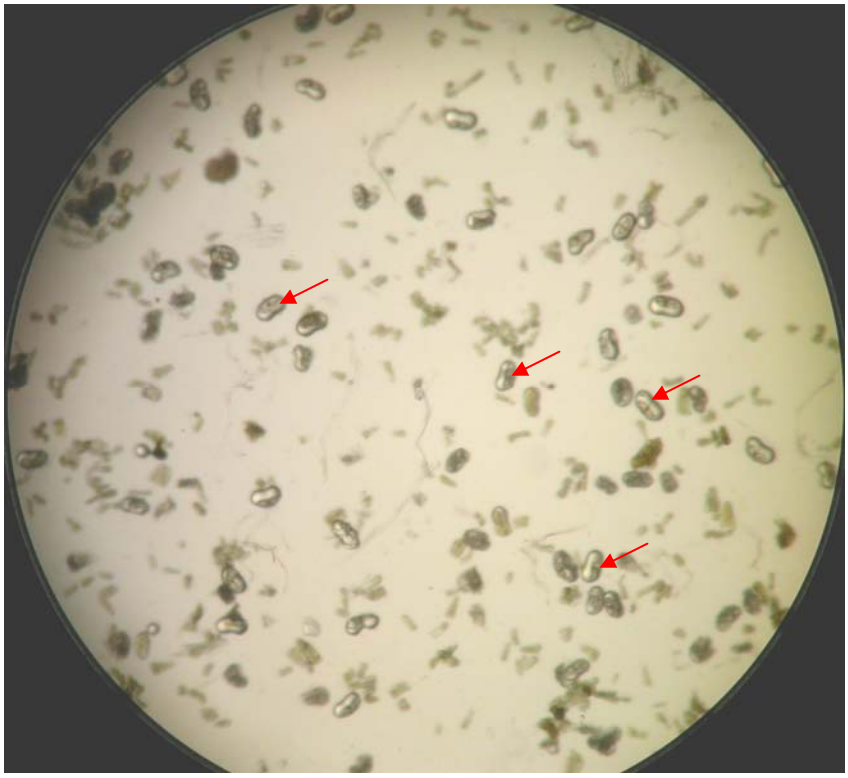

(B)

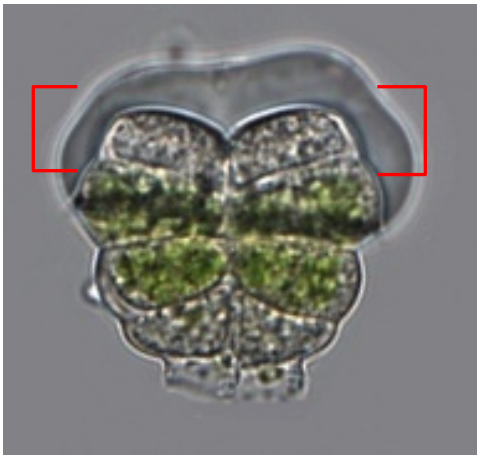

Figure 5.2. (A) Trichome preparation from *A. annua* leaves. Red arrows indicate apical cells with attached cuticular sac. (B) Intact trichome with red brackets denoting the cell clusters pictured in A.

whether or not they were still actively producing terpenoids. Furthermore, the density of the trichomes on floral tissue appeared to be greater than those on the leaf surface. Trichomes were also shown to senesce after anthesis; therefore, it was imperative to harvest the floral buds before senescence occurred (Duke and Paul, 1993). The transfer of plants to a photoperiod of 12 h yielded floral buds after a couple of weeks. Pollen release, anthesis, was observed around day 23 after the plants were transferred to the growth chamber. The presence of free pollen grains in the preparation clogged the filtration mesh and resulted in more fragmented trichomes. With this in mind, a harvest period of 18-20 days after an introduction to a 12 h photoperiod was used. In the first experiments 100 μm beads were used, however it was quickly discovered that they lacked the mass required to break open the floral buds which was necessary to gain access to the trichomes on the inner florets. Therefore, a mixture of 20% 100 μm beads and 80% 500 μm beads (w/w) was used. This yielded better results; however, there were still a lot of fragmented trichomes. Counterintuitively, it was found that increasing the voltage of the Bead Beater reduced the fragmentation of trichomes. In final experiments, the 100 μm beads were found to be extraneous, appearing to only be increasing the degree of broken bead contamination in the trichome preparation. Therefore, it was decided that only 500 μm beads would be used.

A discontinuous Percoll gradient was attempted as previously described for further purification (Slone and Kelsey, 1985). However, potentially due to the differences in buoyant density from the differing amounts of essential oil in the cuticular sacs of the trichomes, good separation was not observed and gradient purification was abandoned. The trichome preparation was deemed acceptable (Figure 5.3) and was further perfected for cDNA library construction by Dr. Thomas Teoh. This involved the determination of optimal rheostat voltage settings, abrasion intervals, and the addition of another filtration step (Teoh *et al.*, 2006).

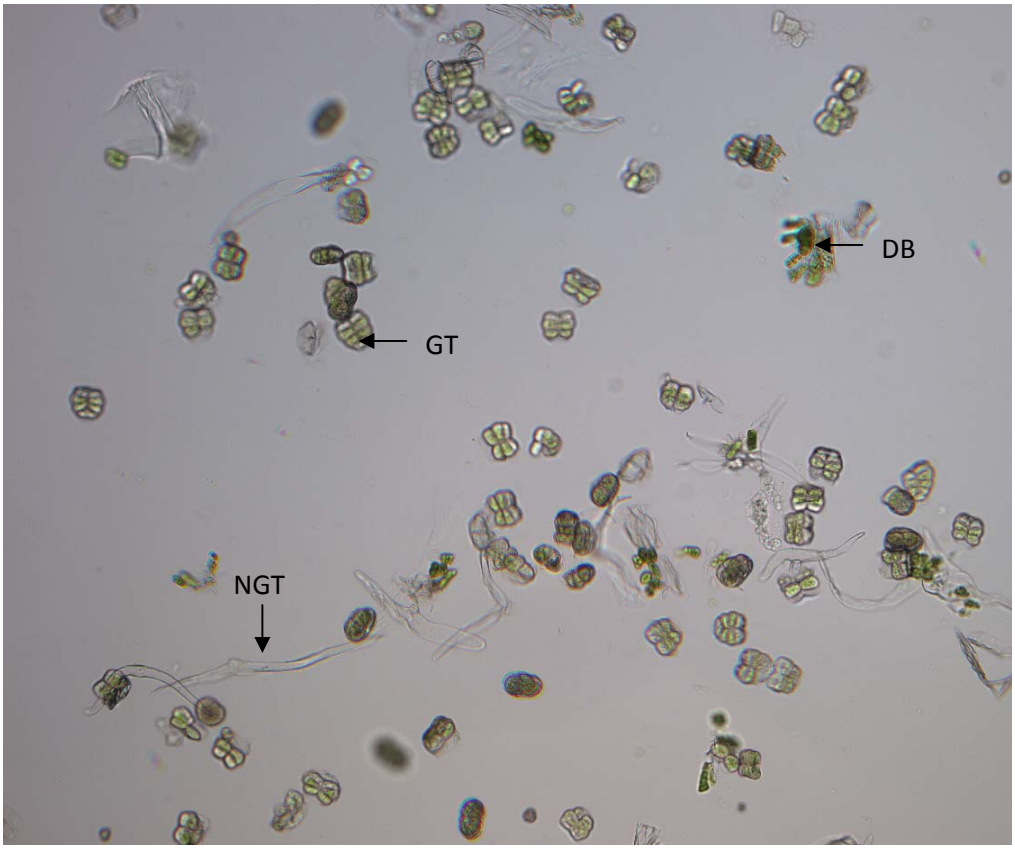

Figure 5.3. Example of an *A. annua* floral bud trichome preparation using the Bead Beater system. GT: glandular trichome; NGT: nonglandular trichome; DB: debris. Reproduced with permission (Covello *et al.*, 2007).

5.2. Gene Expression Analysis

In order to identify a small collection of trichome-specific genes, a set of genes that may be involved in terpenoid metabolism were selected from the trichome cDNA libraries. Since p450, dehydrogenase, and reductase genes were predicted to play a role in artemisinin and monoterpene metabolism we looked for candidate genes in these classes. They were particularly of interest if they were absent from the flower bud library, but were highly represented in the glandular secretory trichome (GST) library and the glandular secretory trichome minus flower bud subtracted (GSTSUB) library (Teoh *et al.*, 2006). These genes, with a preliminarily designated function based on homology, included a cytosolic aldehyde dehydrogenase (*AaALDH1*), an allyl alcohol reductase (*AaDBR1*) , a short chain alcohol

dehydrogenase (*AaMTADH*), the known sesquiterpene cyclase (*AMDS*), and the cytochrome P450 hydroxylase (*CYP71AV1*). As a benchmark for trichome specificity, *AMDS* expression was investigated in root, leaf, floral bud (20 d), and trichome (18-20 d). Since all evidence supports the theory that artemisinin is synthesized in the trichomes, it was decided that *AMDS* was a good candidate for delineating trichome specific expression patterns. Similar experiments were performed using *AaALDH1*, *AaDBR1*, *AaMTADH*, and amorpha-4,11-diene hydroxylase (*CYP71AV1*). The results are shown in Figure 5.4. It is apparent that all of these genes were expressed, to some degree, in trichomes. Faint bands are apparent in the lanes where RNAs from flower bud and leaf tissues were used as template. Since trichomes are ubiquitous on the aerial tissue of *A. annua* one does expect to see signal in most tissues. The observed expression pattern, however, supports the notion that the gene expression is localized to the trichomes since purified trichomes are of a higher density than trichomes on flower buds which are of a higher density than trichomes on leaves. This was observed in the gene expression data. *AaDBR1*, however, seems to exhibit a less trichome-specific expression profile in which isolated trichomes is not the tissue that appears to show the highest expression level. Rather it would appear *AaDBR1* is ubiquitously expressed in the aerial tissues of the plant. This would be indicative of a non-trichome-specific pattern of expression.

5.3. Cell-Specific Gene Expression Analysis

5.3.1. *In situ* Hybridization

A set of genes that appeared to be trichome-specific had been determined by RT-PCR so the next goal was to localize the transcripts to a specific subset of cells within the trichomes.

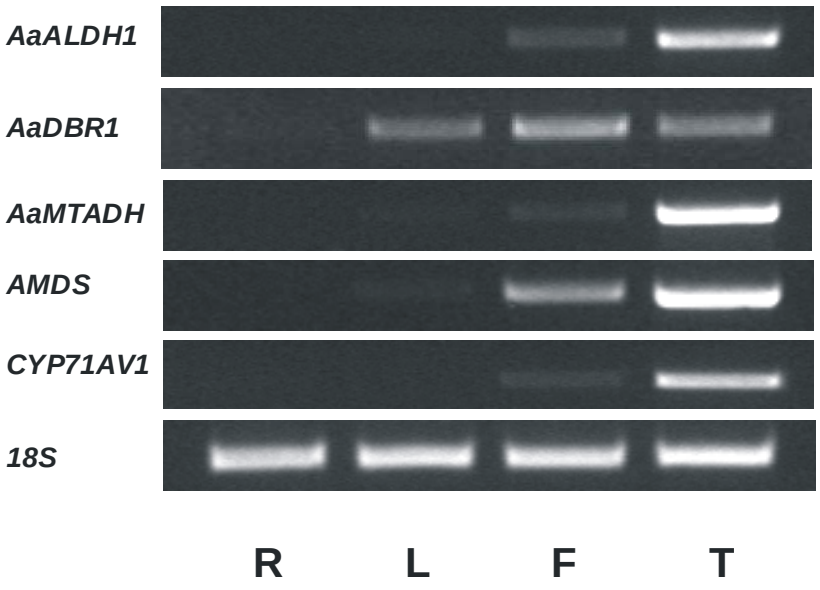

Figure 5.4. Composite of ethidium-bromide stained agarose gels showing the RT-PCR gene expression analysis of *AaALDH1*, *AaDBR1*, *AaMTADH*, *AMDS*, *CYP71AV1*, respectively. 18S is shown as an internal normalization control. *A. annua* plant tissues are denoted as: R- roots, L- leaves, F- floral buds, T- glandular trichomes.

Traditional *in situ* hybridization utilizing paraffin wax embedding (Cox *et al.*, 1988) was attempted on floral buds. The density and semi-ordered nature of the trichomes on the floral buds seemed to suggest that they would be amenable to microtome sectioning. However, although trichomes could be sectioned, usable trichome sections were obtained at a very low frequency (example: 1 sectioned trichome per 5-10 slides of floral bud sections). A picture of a wax embedded section is shown in Figure 5.5. Due to the low frequency of satisfactory sections, it was believed that this technique would not be adequate for localization studies. With those thoughts in mind, it was decided that *in situ* hybridization did not possess the desired efficiency for our studies; therefore, whole mount *in situ* hybridization (WISH) was attempted.

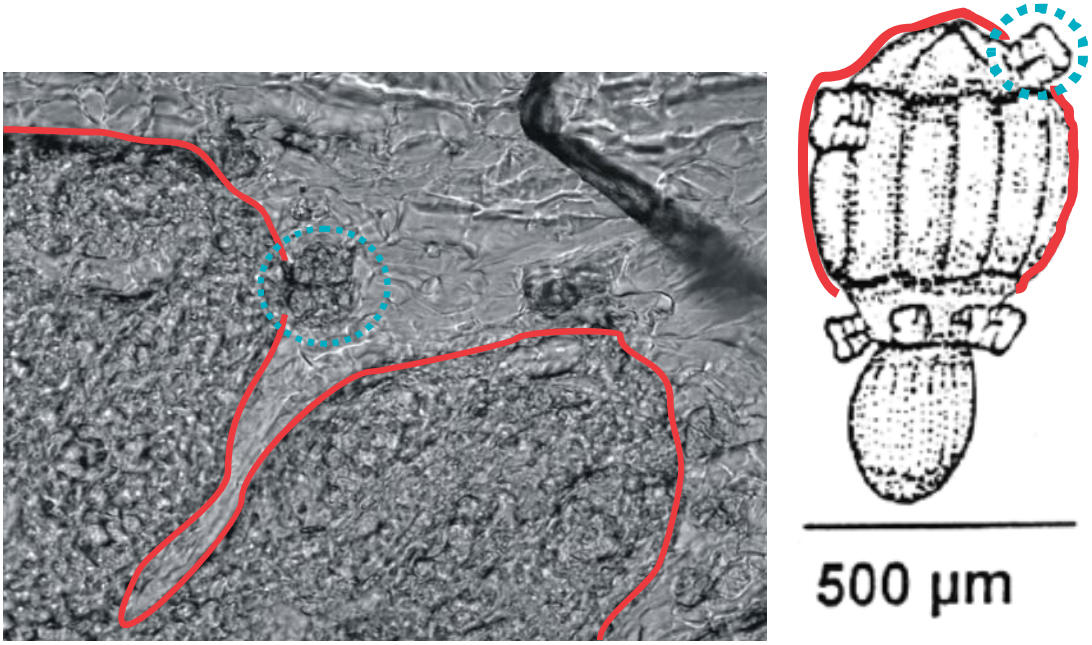

Figure 5.5. Picture of a paraffin wax embedded *A. annua* floral bud section with encircled sectioned trichome. The bud was sectioned longitudinally, in a manner parallel to the glandular trichomes present. Floral bud diagram shows floral bud orientation and an example of an uncut floral bud. Adapted with permission (Ferreira, 1996).

5.3.2. Whole-mount *In situ* Hybridization

Since we possessed a method to obtain relatively pure glandular trichomes, we sought a method to investigate cell-specific gene expression within the trichome. WISH seemed to be perfect for our needs (Engler *et al.*, 1998). WISH was performed on glandular trichomes isolated from floral buds with a probe for amorpha-4,11-diene synthase. The results are shown in Figure 5.6. Two patterns of signal were observed. The 3rd cell pair (from apical) showed signal in most of the trichomes, however, there were some that displayed signal in the 2nd and 3rd cell pairs. These two signal patterns may be caused by developmental differences within the trichome population. The apical 2 cell pairs develop later than the lower cell pairs and may not be active in terpenoid production (Duke and Paul, 1993). Negative controls had no signal in either of those cell pairs. The results obtained were confirmed by two separate hybridization experiments. Probes for other genes involved in the production of terpenoids

were tested (e.g. β-pinene synthase); however, no signal was seen for them (data not shown). This is believed to be due to the low efficiency of WISH rather than the absence of expression. In order for WISH to be successful one must successfully permeablize the cuticle and cell wall of the tissue being analyzed. It may be that the cells of the trichome produce a high amount of essential oil and cuticle which present further barriers to successful penetration.

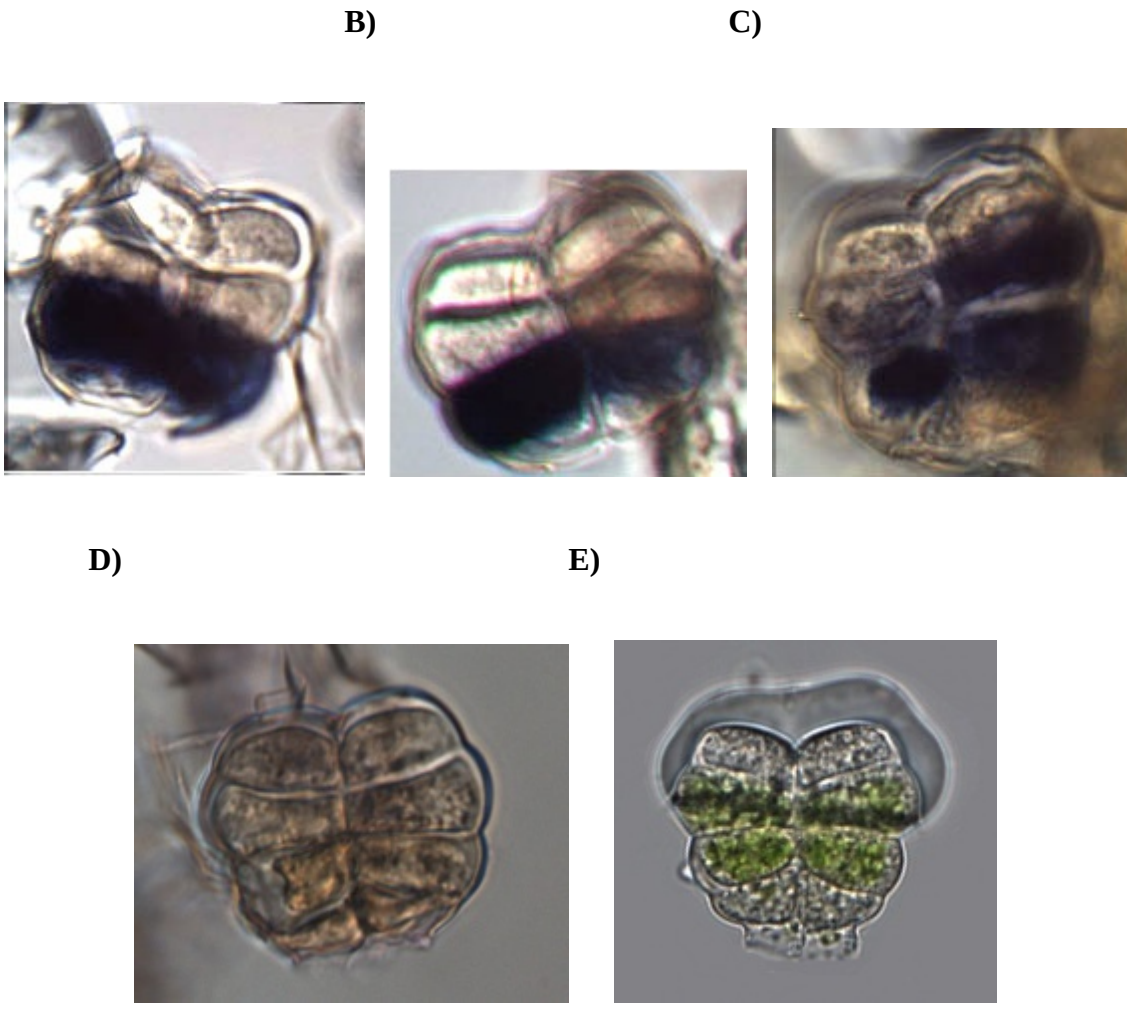

Figure 5.6. Whole mount *in situ* hybridization of isolated *A. annua* glandular trichomes probed for amorpha-4,11-diene synthase. A) Antisense probe showing single cell pair signal (blue). B) Antisense probe showing single cell pair signal. C) Antisense probe showing multiple cell pair signal. D) Sense probe showing no signal. E) Normal trichome for visual reference.

5.4. Isolation of Amorpha-4,11-diene Synthase Promoter

The goal of our promoter isolation was to use the promoter to drive a reporter gene in *A. annua* to confirm our WISH results and to also isolate sequences or factors that control trichome specific gene expression. Using Restriction Site-PCR (RS-PCR), a PCR fragment of ~1.2 kilobases was isolated (denoted as DPPRAMS). The promoter sequence was believed to belong to the *AMDS* gene as part of the *AMDS* ORF was found to be contiguous to the promoter sequence after cloning and sequencing of the amplified fragment. A BLAST search revealed the presence of another sequence submitted by Zhang *et al.* (accession number AY528931) one month earlier. More recently another 4 sequences have been added by Kim *et al.* (accession numbers DQ448294, DQ448295, DQ448296, and DQ448297). However, although there are papers describing *A. annua* transformation, it is highly genotype dependent and even with the appropriate genotype, the plant remains highly recalcitrant similar to most Asteraceae members (Ro, D.K., University of Calgary, personal communication)(Zhang,Y., National Research Council of Canada, personal communication). Efforts to obtain various genotypes were made; however, since there is no commercial supplier, each genotype is the property of a given lab(s) and is not readily disseminated. Therefore, no further work was pursued with the promoter sequence. However, since promoter from our line which produces a low amount of artemisinin does differ in certain positions from the promoter of a line which produces a higher amount of artemisinin (AY528931), it may be of use if indeed the expression of amorpha-4,11-diene synthase is the controlling factor of artemisinin/artemisinic acid accumulation. These sites could be responsible for the difference in flux through the pathway and could be exploited to ensure a high level of expression of amorpha-4,11-diene synthase, or another enzyme in the pathway, for the purposes of metabolic engineering in *A. annua* or a related Asteraceae.

5.5. *A. annua* monoterpene alcohol dehydrogenase

5.5.1. Isolation and sequence analysis

AaMTADH had been shown to be trichome-specific by RT-PCR, suggesting that it may have a role in terpenoid metabolism. To elucidate the function of *AaMTADH*, a heterologous expression approach was undertaken. The glandular trichome (GST) and glandular trichome minus floral bud (GSTSUB) libraries constructed by Dr. Thomas Teoh in our lab revealed a very conspicuous alcohol dehydrogenase (EC 1.1.1.1). It was highly represented in both GST and GSTSUB libraries. This seemed to suggest that the corresponding gene is highly expressed in trichomes. The full length sequence was isolated from the GST library (Figure 5.7) and further sequence analysis was performed to help assign a putative function for this gene. A simple BLASTX search yielded results that were fairly diverse and did not directly hint at any specific function; rather, it merely confirmed that this gene was a member of the short chain alcohol dehydrogenase/reductase superfamily (SDR) (Krozowski, 1994). The top hits with a proposed function found were: *CPRD12* (D88121), a drought inducible gene from *Vigna unguiculata*; *CTS2* (AF286651), a *tasselseed2* homolog in *Cucumis sativus* implicated in male reproductive development and stem secoisolariciresinol dehydrogenase (AF352735), an enzyme that catalyzes the conversion of (-)-secoisolariciresinol into (-)-matairesinol in the phenylpropanoid pathway of *Forsythia x intermedia*. Investigations into known terpenoid dehydrogenases led to isopiperitenol dehydrogenase (*ISPD*) which was described previously (Ringer *et al.*, 2005). As the only characterized terpenoid dehydrogenase that was known to catalyze the oxidation of an alcohol group to an aldehyde/ketone, it was a good example of the type of enzyme we would be expecting to find given the oxidation reactions hypothesized to take place in *A. annua* (Figure 5.8). There was an interesting parallel between ISPD and AaMTADH. It was noted that ISPD had 43% identity (Ringer *et al.*, 2005) and AaMTADH had 51% identity to *Forsythia x intermedia* stem secoisolariciresinol dehydrogenase (FiSDH). ISPD and AaMTADH share only 40% identity to each other. A phylogenetic tree was constructed to examine how AaMTADH related to other plant oxidoreductases (Figure 5.9) (Ziegler *et al.*, 2006). This grouping also suggests that AaMTADH functions as a multimeric enzyme since that cluster of enzymes represents a group of multimeric SDR's. To examine whether all the motifs of an ISPD and FiSDH type SDR were present in AaMTADH, an amino acid alignment of AaMTADH, ISPD and FiSDH was performed and is shown in Figure 5.10. They all share the

conserved dinucleotide cofactor binding, NAG, and YXXXK motifs. The NAG motif aids in cofactor binding and the YXXXR motif participates in substrate oxidation (van der Werf *et al.*, 1999). The catalytic tetrad residues, as well as an aspartic residue, indicative of a preference for NAD+ over NADP+, are also conserved.

```
ATGGCTTCTTTAACTCCAAAAGCAAGATTGGAAAATAAGGTAGCGATTGTCACCGGTGGA
M  A  S  L  T  P  K  A  R  L  E  N  K  V  A  I  V  T  G  G
GCTCGAGGCATCGGAGAATGTATTGTGAGGTTATTCGTAAAACATGGTGCAAAAGTGGTC
A  R  G  I  G  E  C  I  V  R  L  F  V  K  H  G  A  K  V  V
ATCGCTGATGTCAATGACGACCTAGGAAAATTGTTATGCCAAGACTTAGGCTCCAAATTT
I  A  D  V  N  D  D  L  G  K  L  L  C  Q  D  L  G  S  K  F
GCTTGTTTTGTTCATTGTGATGTAACCATTGAGTCTGATATAGAAAATCTCATCAACACC
A  C  F  V  H  C  D  V  T  I  E  S  D  I  E  N  L  I  N  T
ACTATAGCTAAGCATGGACAACTAGATATCATGGTTAACAATGCAGGTACTGTCGATGAG
T  I  A  K  H  G  Q  L  D  I  M  V  N  N  A  G  T  V  D  E
CCAAAACTAAGTATTTTAGATAATGAAAAGTCAGACTTTGATCGTGTGGTAAGCATCAAT
P  K  L  S  I  L  D  N  E  K  S  D  F  D  R  V  V  S  I  N
CTAGCTGGAGTTTTCTTAGGAACAAAACATGCAGCACGTGTGATGATCCCTAAATGTAGT
L  A  G  V  F  L  G  T  K  H  A  A  R  V  M  I  P  K  C  S
GGGAGCATCATCACAACTGCAAGTATATGTTCGGTCACAGGAGGGGTTGCATCTCATGCA
G  S  I  I  T  T  A  S  I  C  S  V  T  G  G  V  A  S  H  A
TACACAAGCTCAAAGCATGGTGTGGTGGGACTTGCAAAGAACGCGGCTGCTGAGCTTGGG
Y  T  S  S  K  H  G  V  V  G  L  A  K  N  A  A  A  E  L  G
AAGTACAATATTCGTGTTAATTGTGTGTCACCTTATTTTGTGCCAACTAAATTAGCATTT
K  Y  N  I  R  V  N  C  V  S  P  Y  F  V  P  T  K  L  A  F
AAATTCTTAAACATGGATGAAACATCAAGTTTTTACTCAAACCTTCAAGGGAAGACACTC
K  F  L  N  M  D  E  T  S  S  F  Y  S  N  L  Q  G  K  T  L
GGACCACAAGATATTGCAAATGCAACCCTTTTTCTAGCAAGTGACGAATCTGGGTATGTA
G  P  Q  D  I  A  N  A  T  L  F  L  A  S  D  E  S  G  Y  V
AGTGGACATAATCTAGTCGTCGATGGTGGCTATAGTGTCCTCAACCCGGCATTTGGTTTA
S  G  H  N  L  V  V  D  G  G  Y  S  V  L  N  P  A  F  G  L
TTTTCATGGAAACCGTAA
F  S  W  K  P  -
```

Figure 5.7. Full length nucleotide sequence of AaMTADH with amino acid translation.

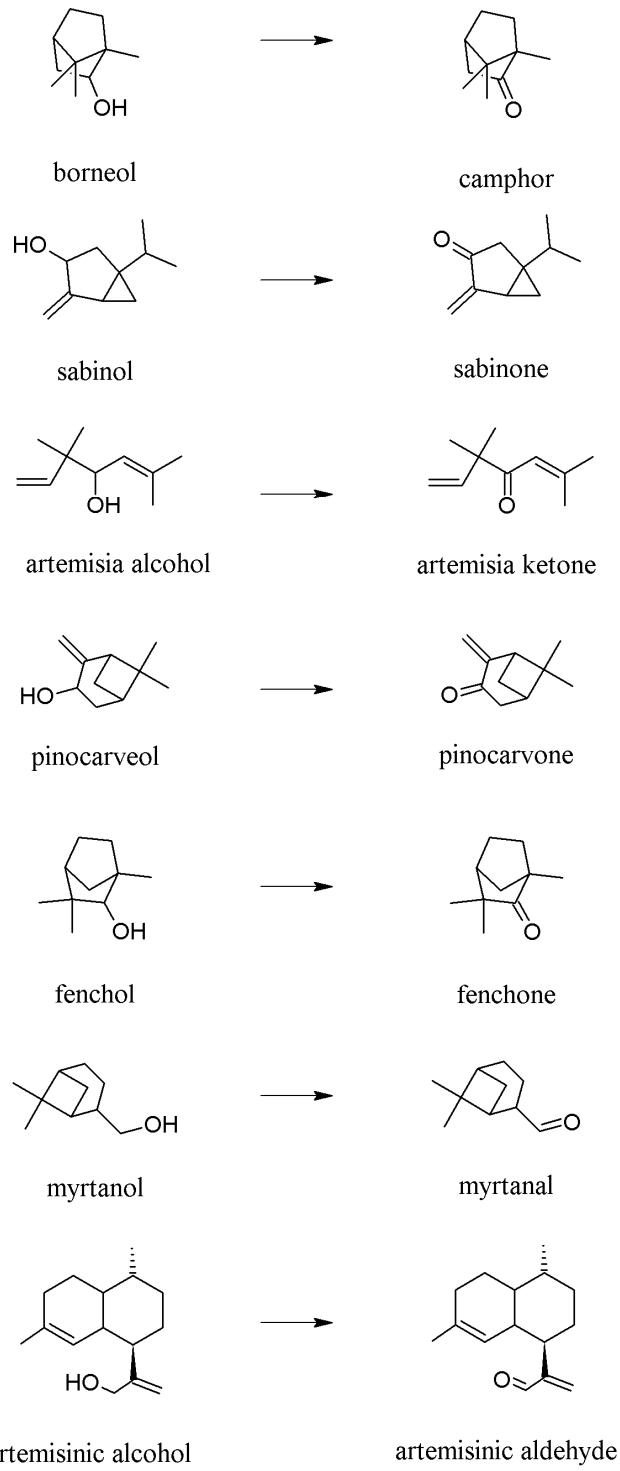

Figure 5.8. Possible oxidative reactions in *A. annua* secondary terpenoid metabolism that could be catalyzed by an alcohol dehydrogenase (Charles *et al.*, 1991; Ferreira *et al.*, 1997; Teixeira da Silva, 2004).

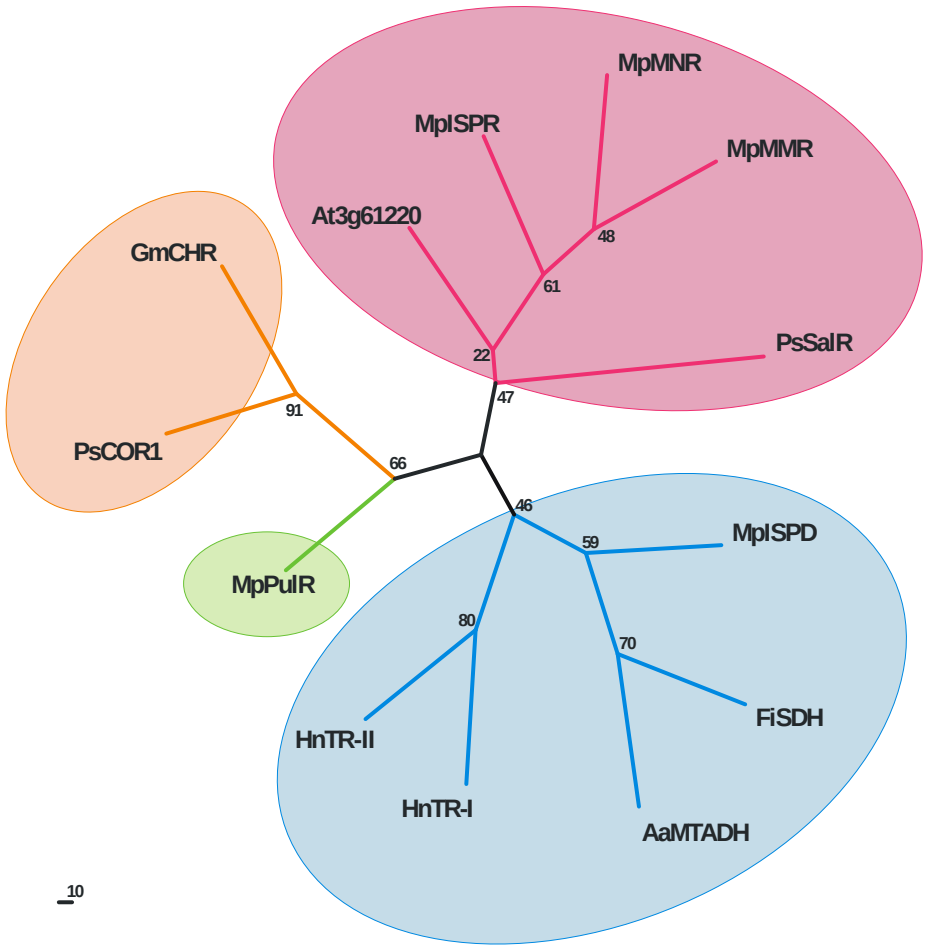

Figure 5.9. Phylogenetic tree of selected oxidoreductase enzymes involved in plant secondary metabolism. The tree was constructed using ClustalW and Phylip available at the Mobyle Web Portal and visualized with TreeView. The blue ellipse outlines the classical 250 amino acid multimeric short chain dehydrogenase/reductase (SDR) group. The pink ellipse outlines the classical 300 amino acid monomeric SDR group. The green ellipse outlines the rare medium chain dehydrogenase/reductase (MDR) superfamily. The orange ellipse outlines the aldo-keto reductase group. The sequences above consist of AaMTADH, monoterpene alcohol dehydrogenase, from *A. annua*; At3g61220 SDR from *Arabidopsis thaliana* that possesses some (-)-menthone:(+)-neomenthol reductase activity, accession NM115986; PsSalR, salutaridine reductase, from *Papaver somniferum*, DQ31621; MpISPR,(-)-isopiperitenone reductase, AY300162; MpMNR, (-)-menthone:(+)-neomenthol reductase, AAQ55959; MpMMR, (-)-menthone:(-)-menthol reductase, AAQ55960; MpPulR, (+)-pulegone reductase, AY300163; MpISPD, (-)-isopiperitenol dehydrogenase, AY641428; which were isolated from *M. piperita*; HnTR-I, tropinone reductase I, D88156; HnTR-II, tropinone reductase II, L20485; both of which were from *Hyoscyamus niger*; FiSDH, secoisolariciresinol dehydrogenase, from *Forsythia x intermedia*, AAK38665; PsCOR1, codeinone reductase 1, from *Papaver somniferum*, AF108432; GmCHR, chalcone reductase, from *Glycine max*, X55730. Bootstrap value used was 100. (Ziegler *et al.*, 2006)

Figure 5.10. Amino acid sequence of AaMTADH aligned with ISPD (AY641428) and FiSDH (AAK38665). The nucleotide cofactor binding motif (Motif I), the NAG site (Motif II), and the active site element YXXXK (Motif III) are underlined. The asterisk denotes the conserved aspartate residue that is an indication of a nucleotide cofactor preference for NAD(H). The arrows indicate the catalytic tetrad residues. Black boxes indicate identical residues in 2 or more sequences, grey boxes indicate similar residues. Sequences were aligned with CLUSTALW and displayed using BOXSHADE Server.

5.5.2. Purification of AaMTADH

Heterologously expressed AaMTADH was purified from cleared *E. coli* lysate using a 6X His-tag and a nickel column. The eluent was desalted to remove imidazole, which yielded a partially pure protein that was deemed to be ~85% pure and appropriate for the substrate and kinetic studies (Figure 5.11). This protein was then utilized for testing the activity of AaMTADH.

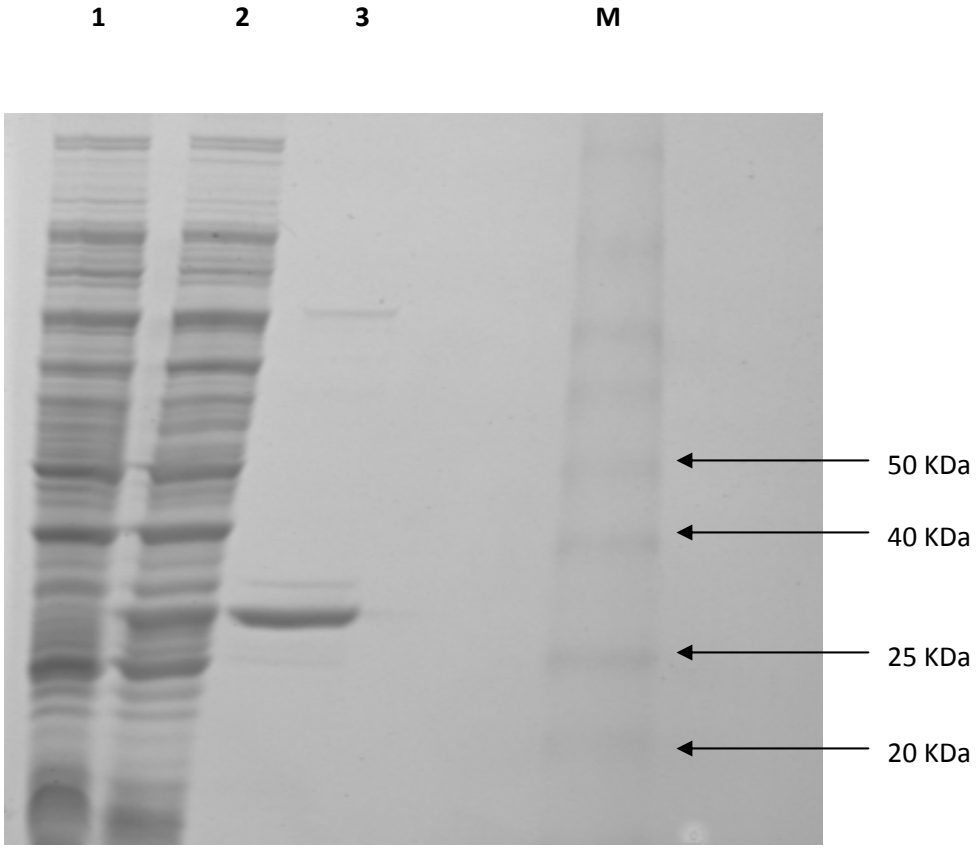

Figure 5.11. SDS-PAGE gel of AaMTADH HIS-Tag purification. Lane 1: Crude lysate of pET15b (empty vector) containing *E. coli* induced with IPTG; Lane 2: Crude Lysate of pDP001 (pET15b::AaMTADH) containing *E. coli* induced with IPTG; Lane 3: His-Tag purified AaMTADH; Lane M: Prestained protein marker (Bio-Rad).

5.5.3. Characterization of AaMTADH

AaMTADH was tested with various substrates found in *A. annua*. Figure 5.12 shows the gas chromatogram of the AaMTADH catalyzed reaction of artemisia alcohol to artemisia ketone. The other possible monoterpene substrates were tested in a similar manner (Figures 5.13 to 5.18). Artemisia alcohol, borneol, *c*/*t*-pinocarveol, and fenchol are oxidizable substrates of this enzyme. Artemisinic alcohol and myrtanol, both primary alcohols instead of secondary alcohols like the other substrates previously mentioned, are not oxidized by AaMTADH. Difficulties were encountered with sabinol extraction from assay samples and it is therefore impossible to conclude with confidence that it is being oxidized to sabinone by

AaMTADH. However, there does seem to be an increase in the peak height of sabinone in relation to sabinol in comparison to the reaction lacking AaMTADH (data not shown).

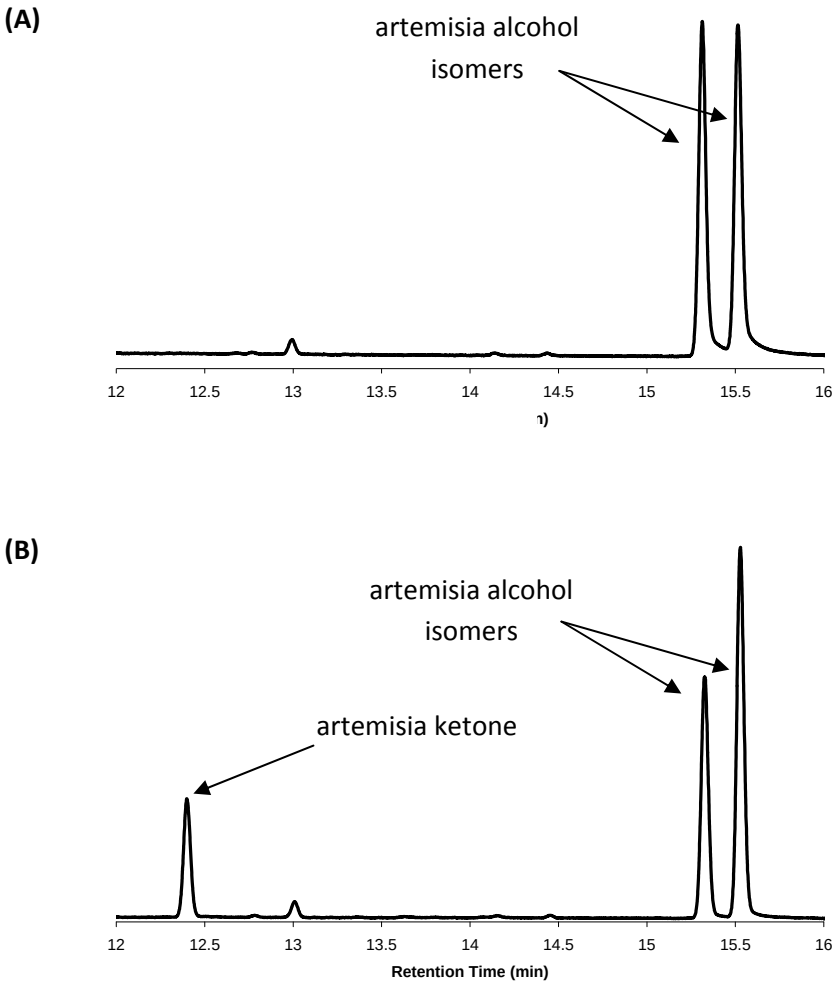

Figure 5.12. GC Flame Ionization Detector (FID) traces of AaMTADH dehydrogenase assays utilizing racemic artemisia alcohol as the substrate. (A) Negative control reaction lacking AaMTADH enzyme. (B) Reaction complete with AaMTADH enzyme. This reaction was analyzed using a chiral GC column.

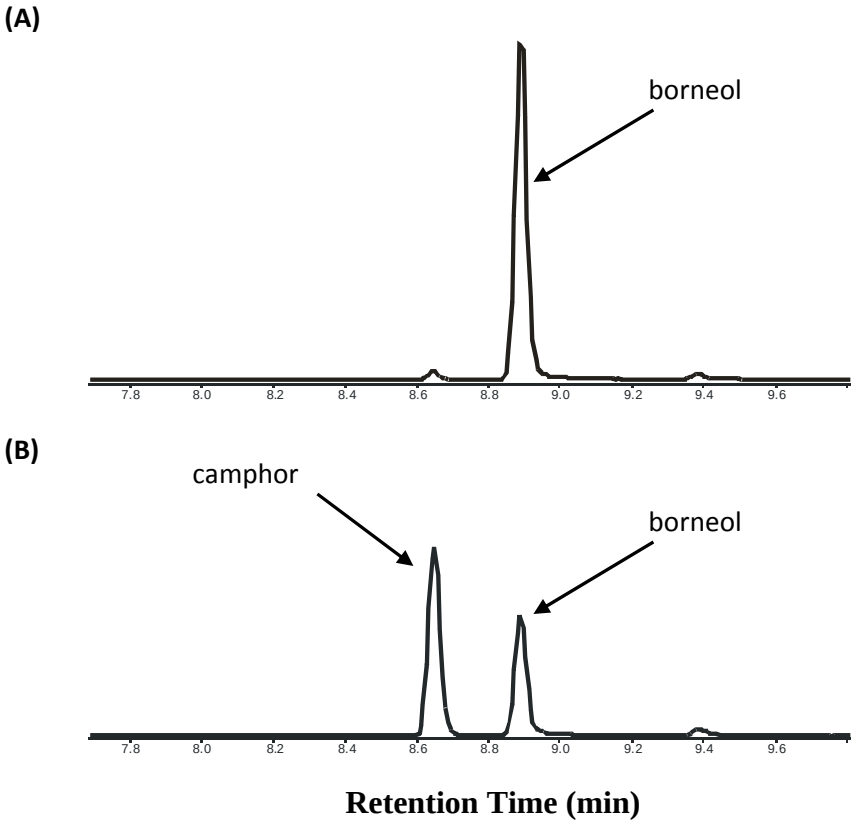

Figure 5.13. GC Total Ion Count (TIC) traces of AaMTADH dehydrogenase assays utilizing borneol as the substrate. (A) Negative control reaction lacking AaMTADH enzyme. (B) Reaction complete with AaMTADH enzyme. This reaction was analyzed using a DB5 GC column.

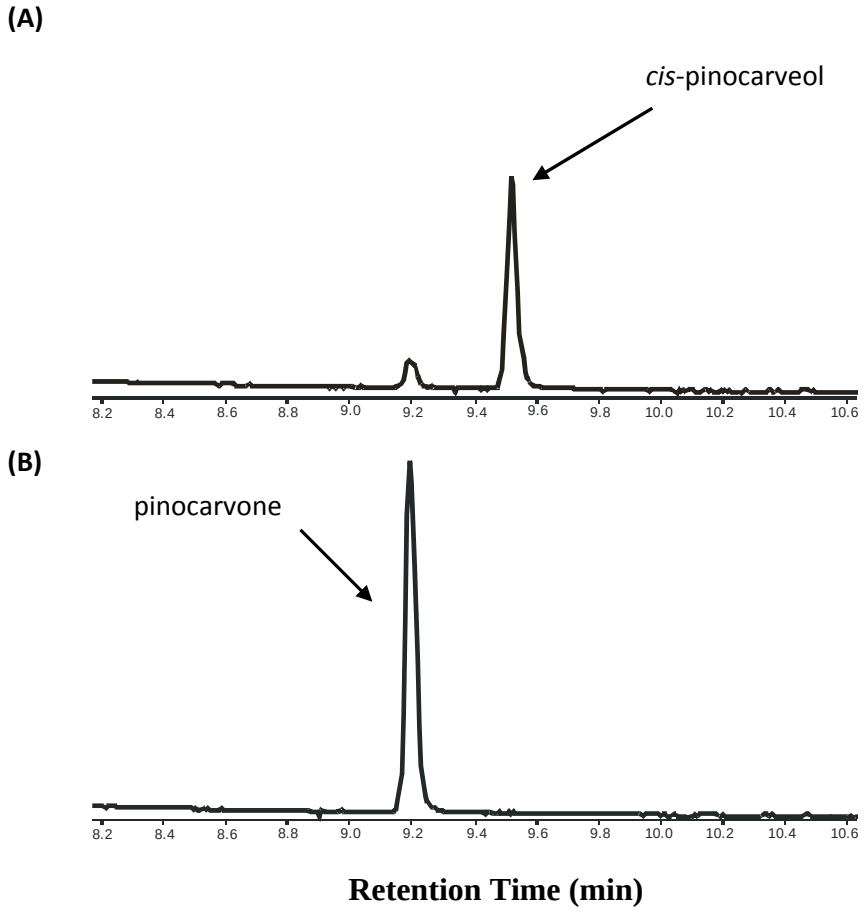

Figure 5.14. GC Total Ion Count (TIC) traces of AaMTADH dehydrogenase assays utilizing *cis*-pinocarveol as the substrate. (A) Negative control reaction lacking AaMTADH enzyme. (B) Reaction complete with AaMTADH enzyme. This reaction was analyzed using a DB5 GC column.

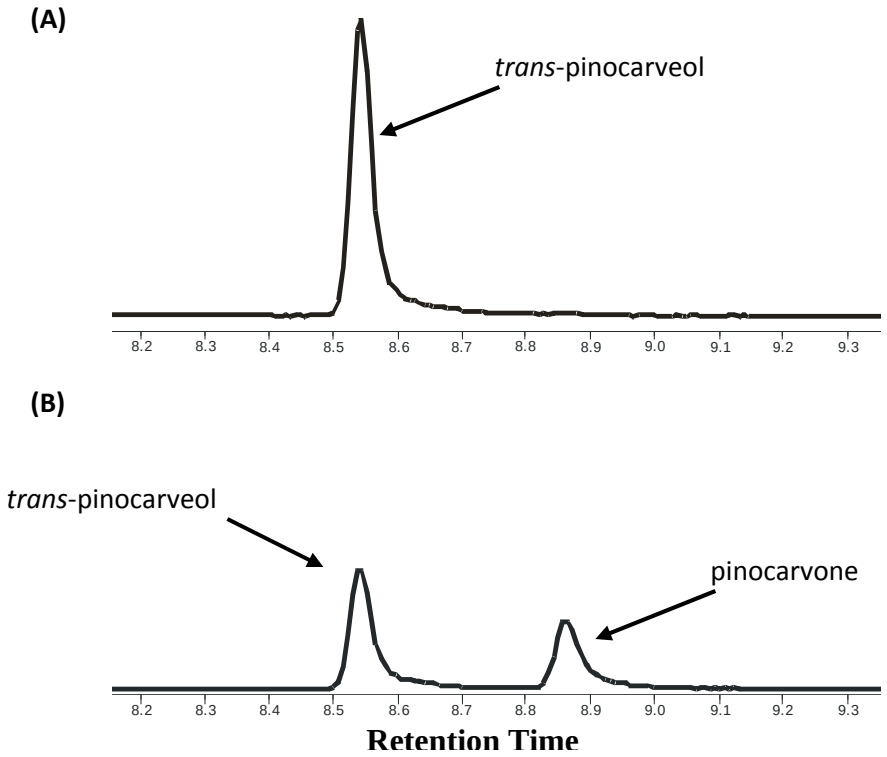

Figure 5.15. GC Total Ion Count (TIC) traces of AaMTADH dehydrogenase assays utilizing *trans*-pinocarveol as the substrate. (A) Negative control reaction lacking AaMTADH enzyme. (B) Reaction complete with AaMTADH enzyme. This reaction was analyzed using a DB5 GC column.

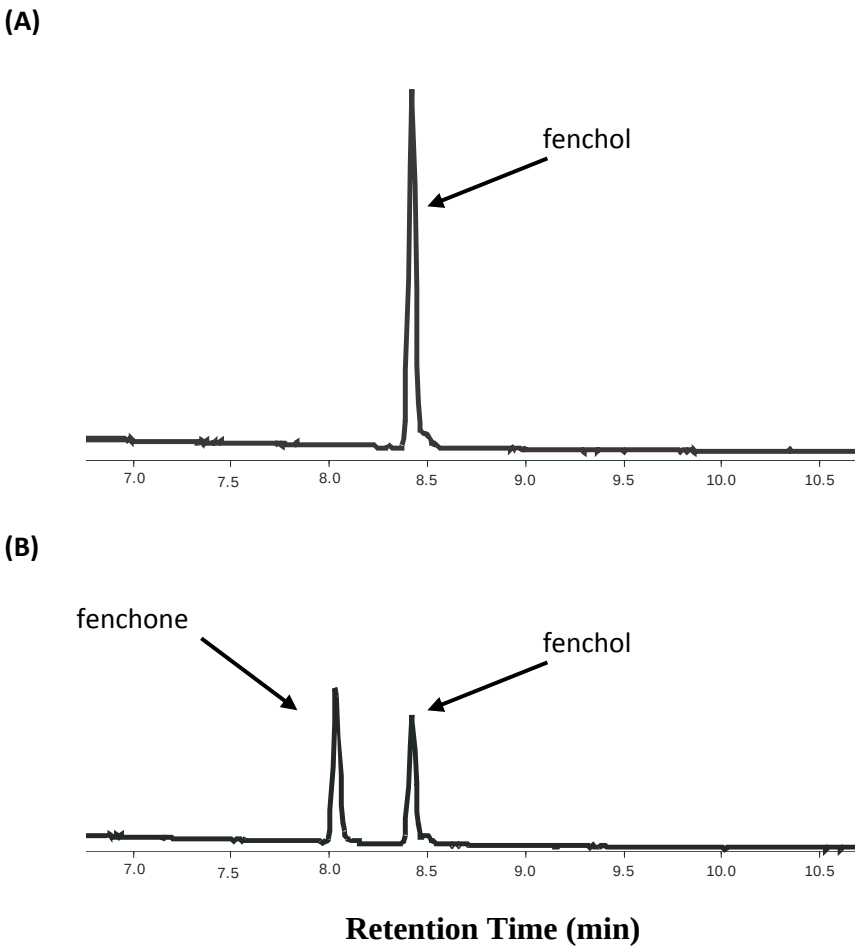

Figure 5.16. GC Total Ion Count (TIC) traces of AaMTADH dehydrogenase assays utilizing fenchol as the substrate. (A) Negative control reaction lacking AaMTADH enzyme. (B) Reaction complete with AaMTADH enzyme. This reaction was analyzed using a DB5 GC column.

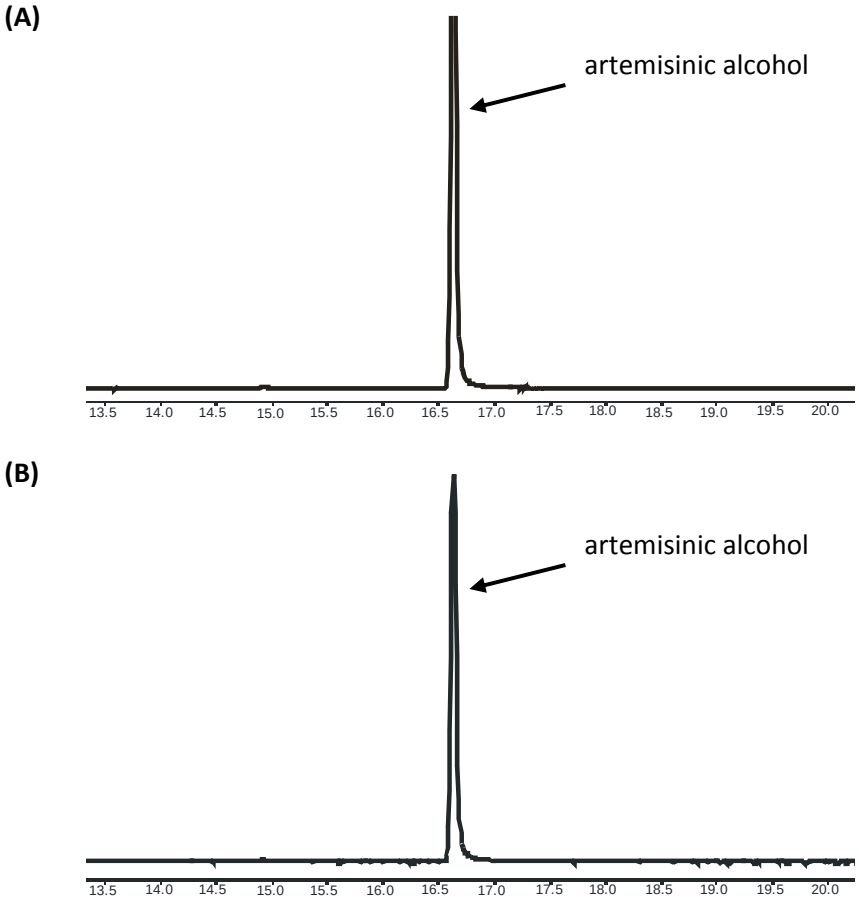

Figure 5.17. GC Total Ion Count (TIC) traces of AaMTADH dehydrogenase assays utilizing artemisinic alcohol as the substrate. (A) Negative control reaction lacking AaMTADH enzyme. (B) Reaction complete with AaMTADH enzyme. This reaction was analyzed using a DB5 GC column.

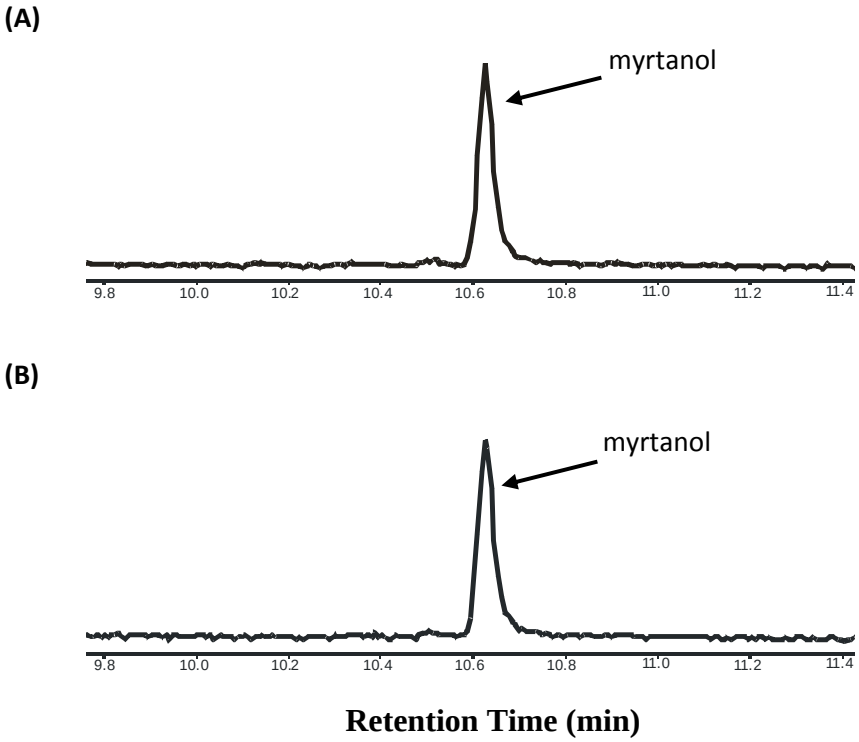

Figure 5.18. GC Total Ion Count (TIC) traces of AaMTADH dehydrogenase assays utilizing myrtanol as the substrate. (A) Negative control reaction lacking AaMTADH enzyme. (B) Reaction complete with AaMTADH enzyme. This reaction was analyzed using a DB5 GC column.

The enzyme appears to exhibit a preference for certain stereoisomers. Cis-pinocarveol appears to be quite readily oxidized, although, trans-pinocarveol is the isomer seen in the essential oil. The artemisia alcohol substrate used in this study was racemic at the hydroxyl position since it was created by the chemical reduction of artemisia ketone. GC analysis with a chiral column revealed that AaMTADH seemed to be catalyzing the conversion of only one of the isomers, or had a distinct preference for one isomer over the other. As borneol and pinocarveol are the only substrates commercially available with known purity and stereochemistry, these along with artemisia alcohol, were used in further kinetic analyses.

The pH optimum of AaMTADH was determined using a 5 minute reaction time at which time the reaction with artemisia alcohol was still linear (Figure 5.19). A pH optimum of ~10.0 was observed, which is similar to the pH of 10.0 reported for ISPD and within range expected for short chain alcohol dehydrogenases (Figure 5.20) (Ringer *et al.*, 2005).

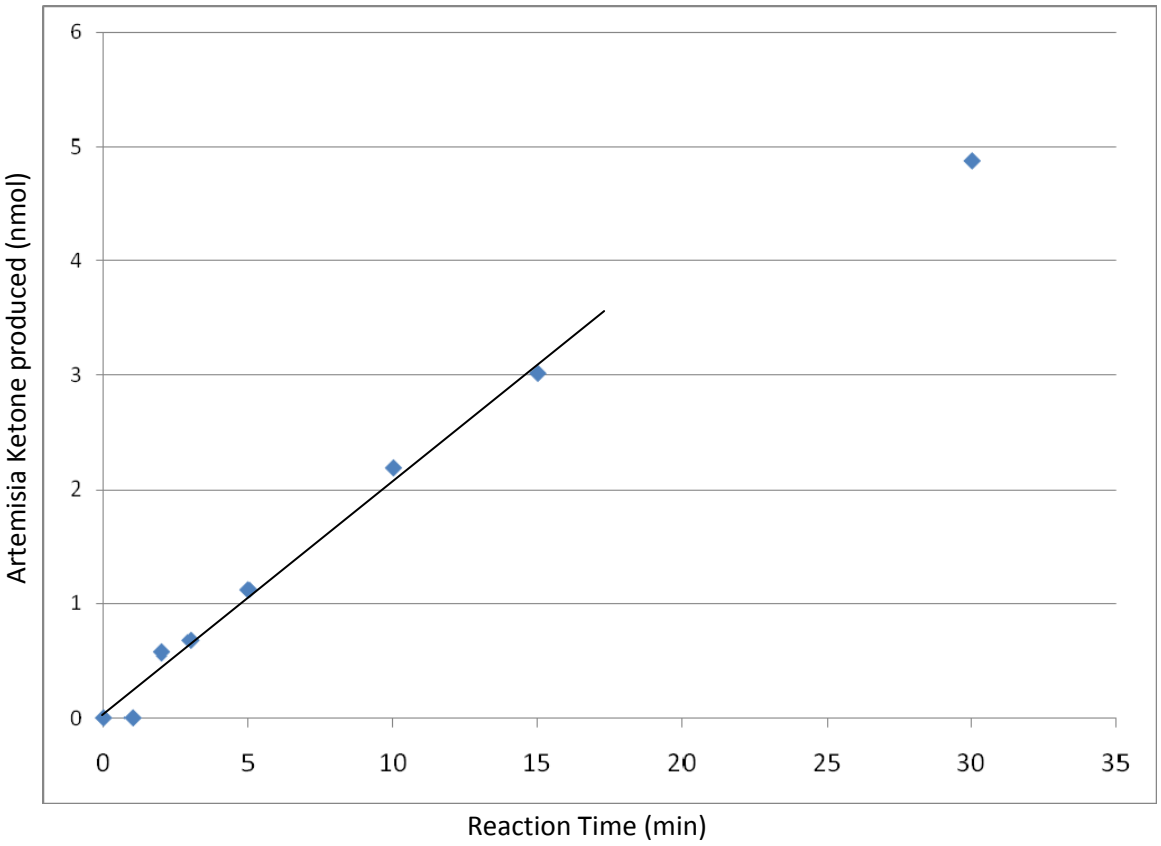

Figure 5.19. Analysis of the reaction linearity of AaMTADH with artemisia alcohol. Reactions were incubated for 0, 1, 2, 3, 5, 10, 15, and 30 min at 30°C and stopped by the addition of ethyl acetate.

It was indicated by the conserved Asp residue that this enzyme had a preference for NAD+ over NADP+; however, to be certain we tested this with artemisia alcohol (Figure 5.21). NAD+ was clearly the preferred coenzyme.

Kinetic experiments were attempted but did not yield acceptable results in time for the publishing of this thesis. However, the partial characterization that was achieved for AaMTADH provides essential information which will aid a full kinetic evaluation of the enzyme in the future. This information also gives insight into *A. annua* monoterpene biosynthesis and possible classes of enzymes involved.

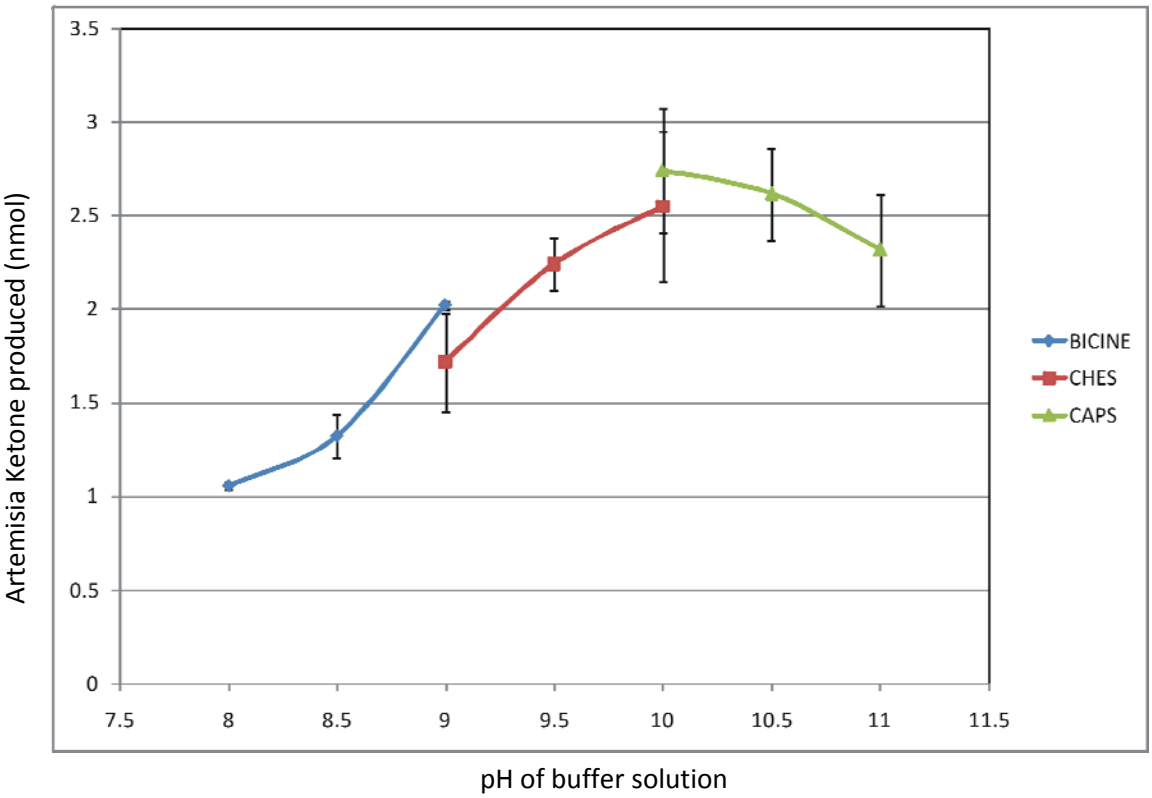

Figure 5.20. Determination of the pH optimum of AaMTADH with artemisia alcohol. The graph is an average of 3 replicates with standard deviation shown with error bars. The pH range used was from 8-11 using bicine (pH 8-9), CHES (pH 9-10), and CAPS (pH 10-11) buffers. Reactions were incubated at 30^{o}C and stopped with the addition of ethyl acetate.

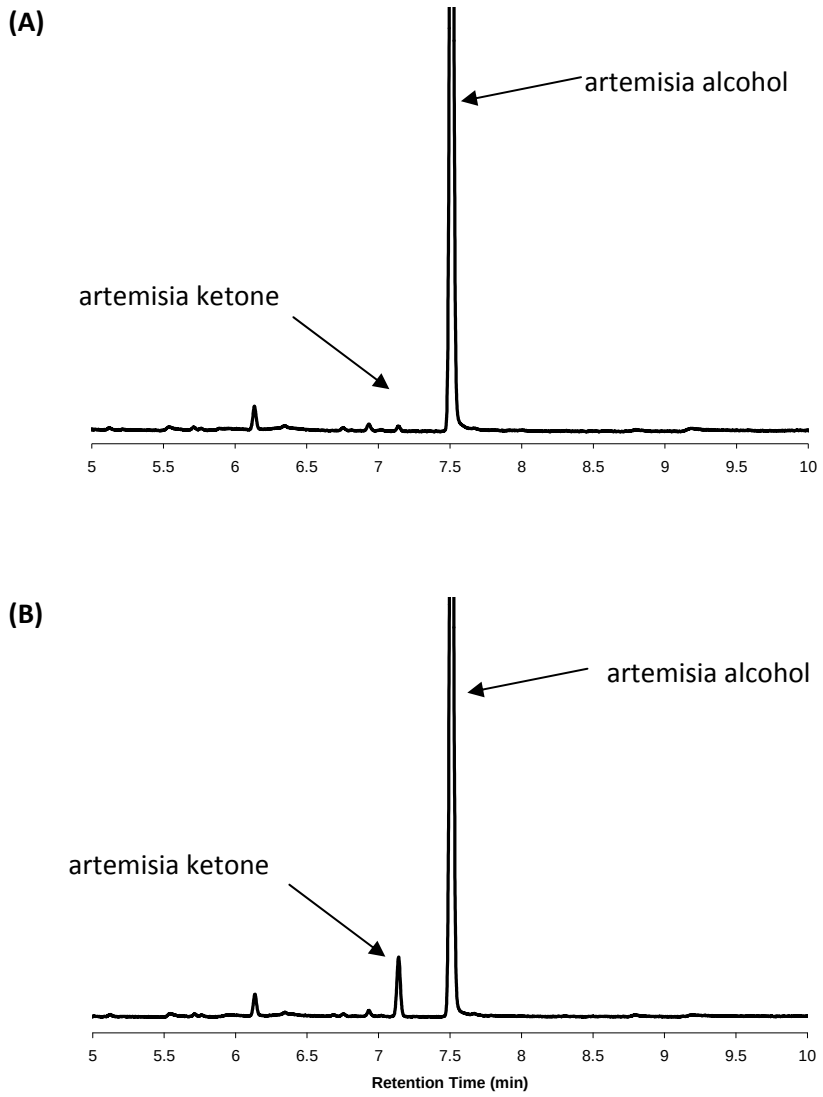

Figure 5.21. GC FID traces of a coenzyme dependency assay of AaMTADH and artemisia alcohol using either NADP+ (A) or NAD+ (B). This reaction was analysed using a DB-5 GC column.

6. DISCUSSION

A. annua glandular trichomes have been studied to a fair degree using light and electron microscopy techniques (Duke *et al.*, 1994; Duke and Paul, 1993). However, almost no research regarding the biochemistry and expression of genes within the glandular trichome has been performed. In this study, we aimed to obtain a relatively pure population of glandular trichomes that could be used to analyze terpenoid biosynthesis in *A. annua*. In order to gain a better understanding of the glandular trichomes of *A. annua*, tissue and cell-specific expression patterns for terpenoid biosynthetic genes were investigated and a gene with function in monoterpene metabolism was isolated.

6.1. Trichome Isolation

In order to effectively isolate genes of a putative function, it is very useful to be able to use cell/tissue specific expression patterns to delineate a subset of possible candidates. The Beadbeater technique provides a highly efficient means of isolating trichomes for numerous species of plants for the purpose of RNA/protein analysis. Successful implementation of this technique has been reported with *M. piperita*, tansy, and other plant species (Gershenzon *et al.*, 1992; Lange *et al.*, 2000). The peltate trichomes of mint, and similarly capitate trichomes found in tobacco, are more readily amenable to this technique. The biseriate trichomes found in tansy and *A. annua* present a special challenge in comparison. They do not possess a slender stalk which can be easily broken. As well the secretory cells do not appear to be packaged in the form of a disc or globular cluster as in *M. piperita* or *N. tabacum* (Akers *et al.*, 1978; Duke and Paul, 1993; Turner *et al.*, 2000a). In *A. annua*, it appears that the flowers provide the ideal tissue as the base of the trichome is not indented into the epidermis as it is on the surface of the leaf. In our investigation, we have shown that this technique is applicable to *A. annua* trichomes and most likely other Anthemideae tribe members. One of the most useful attributes of *A. annua* which may not be found in other Anthemideae members is its photoperiod-dependent flowering. This means that one can easily obtain developmentally similar flowers/trichomes easily, instead of having to endure the difficulties associated with harvesting and storing tissue which random flowering times would require.

Furthermore, the significance of using flower tissue that provides highly accessible, dense glandular trichomes with an absence of nonglandular trichomes was clearly demonstrated in our studies. In the study by Gershenzon *et al.* (1992) there was no mentioning of flower tissue in the brief reference to tansy trichome isolation so one may assume this protocol was tested primarily on leaf tissue. While the use of flower tissue helps to eliminate contamination of the preparation from nonglandular trichomes, a new source of contamination is encountered, namely pollen. In our studies, pollen severely affected the integrity and quantity of the trichome preparation and hence attention should be paid to minimize the extent of any contamination. This would require testing flowers of various stages of development as floral integrity and not just anthesis seemed to determine the extent of pollen contamination. In order to study other species such as *Tanacetum parthenium*, which possess larger flowers, it may be necessary to physically break up the flower before attempting to isolate the glandular trichomes from the tissue. *A. annua* flowers are only 1-3 mm in diameter and were easily broken up by the 500 μm beads. Any such difficulties, however, must be overcome because the advantages of using an isolated trichome preparation over one derived from whole flower or leaf tissue for molecular genetics work cannot be overstated. In order to accurately and efficiently study a cell/tissue specific natural product pathway, the separation of those cells/tissues from non-producing tissues is paramount.

6.2. Gene Expression Analysis

The RT-PCR analysis of the expression patterns of *AaALDH1*, *AaMTADH*, *AMDS*, and *CYP71AV1* revealed that these genes are primarily expressed in the glandular trichomes of *A. annua* suggesting that they were involved in terpenoid metabolism. The enzymatic activity of AMDS was already determined before our study, so it served as the standard for a terpenoid metabolism related gene with trichome localization. A dissimilar pattern of expression was found for *AaDBR1*, which suggests it does not share a terpenoid biosynthetic function. In subsequent experiments performed with these genes (Teoh and Zhang, National Research Council of Canada, unpublished work)(Teoh *et al.*, 2006), AaALDH1 and CYP71AV1 were shown to be involved in artemisinin biosynthesis. AaDBR1, however, was

shown to be a 2-alkenal reductase which suggests it may be involved in the detoxification of the 2-alkenal products of lipid photo-oxidation (Mano *et al.*, 2005). This function correlates well with the fairly ubiquitous aerial tissue expression observed. Therefore, it can be concluded that genes that are highly expressed in *A. annua* trichomes have a probability of being involved in terpenoid production. However, even if a given gene of interest has the same expression profile as AMDS, it still only suggests the given gene may have a role in terpenoid metabolism. Heterologous expression of the gene of interest would still be needed to determine what role, if any, the gene possesses.

6.3. Trichome Biology

The three main glandular trichome morphologies that are commonly encountered are peltate, capitate, and biseriate. The first two are seen in *M. piperita* and possess the basic structure features one would expect in a trichome. There is a cuticular sac at the apex to hold the essential oil, a cluster of cells beneath that to synthesize the essential oil, and a number of stalk cells underneath that raise the trichome off the surface of the leaf. However, the biseriate trichomes of Artemisia spp. depart from this structural scheme. The apex still retains the cuticular sac and there are cells that help raise the trichome off the leaf surface; however, the cells that appear to be synthesizing amorpha-4,11-diene and perhaps other terpenoids, are not directly beneath the sac. Instead they appear to be the cluster of green cells that exist under a pair of apical nongreen cells. This was indicated by the WISH results using a probe for the first gene of the artemisinin biosynthetic pathway, amorpha-4,11-diene synthase. This is the first cell-specific localization of any terpenoid related gene in a biseriate trichome. Other terpenoid biosynthesis related genes may reside in other cell pairs. Our WISH data, combined with ultrastructure studies (Duke and Paul, 1993) showing both cuticular expansion encompassing the apical 3 cell pairs and exudate within the apical 3 cell pairs strongly suggests that apical three pairs of cells constitute the secretory head in *A. annua* trichomes (Duke and Paul, 1993; Turner *et al.*, 2000a; Wagner, 1991). Whether there is any spatial separation of mono- and sesquiterpene pathways or of any of the genes in the artemisinin pathway needs to be investigated further with ISH or immunohistochemical analyses utilizing

all of the known terpenoid related genes in *A. annua*. Such a model is possible since all three cell pairs have been structurally evaluated as biosynthetically competent (Duke and Paul, 1993). Even the transport of essential oil out of the cells and into the cuticular sac remains uncertain as the cuticular sac appears to encompass the 3 apical cell pairs. Previous studies have shown that essential oil appears to accumulate at the apex of the gland (Duke and Paul, 1993). If the oil does only accumulate at the apex of the gland, this suggests that perhaps amorpha-4,11-diene or other terpenoids are being transported through 2 more cell pairs in their journey to being transformed into one of the chemical constituents of the essential oil. If the essential oil does go through the other apical cell pairs it is possible that the constituents are modified as they are transported to the cuticular sac. Perhaps there is a spatial separation of enzymes in the terpenoid biosynthetic pathways. On the other hand, it is also possible since the cuticular sac encompasses the apical 3 cell pairs that the cells directly secrete the essential oil into the cuticular sac. If those cells do secrete essential oil directly into the subcuticular space, that may suggest that apical cell pair and the sub-apical green cell pairs have different functions as they possess different morphologies (Duke and Paul, 1993). One possible function of the chloroplast containing cells may be to supply the trichome with photosynthate with which to synthesize terpenoids. However, since we see AMDS expression in those cells, we know they must also play some direct role in terpenoid biosynthesis. There are still many unanswered questions remaining about the biosynthesis and transport of terpenoid compounds in the trichomes of *A. annua*. Are mono- and sesqui-terpenes biosynthesized in the same cell pairs? Which cell pairs are secreting terpenoids into the subcuticular space of the trichome? Further investigations will help to address these questions.

The localization of AMDS within the trichome and the isolation of the AMDS promoter will allow for engineering of the trichome in the Asteraceae family. It will allow for the expression of other terpenoid modifying enzymes to alter the composition of the essential oil as desired. Alternatively, compounds not even found in trichomes under normal circumstances could be produced taking advantage of the trichome's attributes (Schilmiller *et al.*, 2008). Whether transportation mechanisms exist that would be amenable to the production of compounds of interest remains to be seen. Crop enhancements could be made

to such biseriate trichome bearing plants as sunflower and chrysanthemum, allowing for increased pest resistance via modified essential oil composition. Some scientists have even speculated about the use of trichomes as factories for biofuels and pharmaceuticals (Schilmiller *et al.*, 2008).

6.4. *A. annua* Monoterpene Alcohol Dehydrogenase and Trichome-specific Genes

The EST's derived from the isolated glandular trichomes were shown to be very rich in isoprenoid metabolism. Some of the most abundant transcripts were amorpha-4,11-diene synthase, amorpha-4,11-diene mono-oxygenase, various monoterpene synthases, and AaMTADH. This demonstrates the advantag of using isolated trichomes from *A. annua* for the purpose of investigating terpenoid biosynthesis and suggests the biosynthetic nature of the biseriate trichomes. Since the variety of *A. annua* we used was high in monoterpenes it is logical that we observed a high representation of AaMTADH. However, in another EST library from a line of *A. annua* that does not possess high amounts of monoterpenes, AaMTADH ESTs were absent (Zhang, National Research Council of Canada, unpublished results).

Alcohol dehydrogenases are known to be promiscuous enzymes (Krozowski, 1994) and MTADH does not differ as it appears to be active with most of the reported monoterpenes in *A. annua*. Therefore, it is possible to assume that AaMTADH is responsible for all of these monoterpene alcohol oxidations *in vivo* (Figure 5.8). AaMTADH's main substrates within the trichome would most likely be borneol and artemisia alcohol as their ketone products are high in the essential oil of *A. annua* (Charles *et al.*, 1991; Teixeira da Silva, 2004). It possesses a pH optimum of 10.0 which is similar to the reported optimum for ISPD. If rls></urls></record></Cite></EndNote> (Gershenzon et al., 1992) .
es of A. annua seemed to be amenable to this protocol as they too were protruding from the
A high pH optimum is not unexpected in enzymes that oxidize alcohols as the alkaline pH shifts the reaction equilibrium in favour of aldehyde/ketone formation. A high pH, however, adversely affects enzyme stability which then lowers enzyme activity (Worthington, 1993).

The promiscuity of AaMTADH may suggest that a vast array of monoterpenes can be produced with only a few enzymes. Cyclases which are capable of producing more than one carbon skeleton, have been previously indentified (Bohlmann *et al.*, 1998; Withers and Keasling, 2007). Alcohol dehydrogenases like AaMTADH which can oxidize more than one monoterpenol, could then oxidize those various carbon skeletons. This suggests that if one wishes to modify the essential oil composition of a given aromatic plant, one may have to employ a directed evolution approach to achieve the desired results. In using such a strategy one might be able to evolve an enzyme which only produces one product. This may be necessary because there may only be a very small number of enzymes involved in determining the diversity of terpenoids within the essential oil.

At the time of writing, the only other related monoterpene dehydrogenase that has been isolated has been isopiperitenol dehydrogenase (ISPD) from *M. piperita*. This enzyme also possesses a slightly promiscuous nature, showing activity on carveol and isopiperitenol. However, since no comprehensive substrate screen was ever conducted, the true catalytic spectrum cannot be surmised. The interesting commonality shared between these two enzymes is their identity to secoisolariciresinol dehydrogenase, which is part of the lignan pathway and seemingly far removed from isoprenoid metabolism. How these plants evolved so that an enzyme from lignan metabolism became recruited to trichomes to fulfill a role in a fairly dissimilar chemical environment is truly mysterious. It is interesting, however, that this enzyme did not possess any activity towards primary alcohols, in particular towards artemisinic alcohol. There were no other similar dehydrogenases found in the library. This leaves two possibilities: CYP71AV1 is the enzyme that is responsible for further oxidations of artemisinic alcohol (Ro *et al.*, 2006; Teoh *et al.*, 2006) or there is a completely dissimilar dehydrogenase responsible for that function. The latter idea is not unreasonable as there exists a high tolerance for sequence divergence within the family (Krozowski, 1994). This suggests a dehydrogenase may have the same activity as another dehydrogenase, but a dissimilar amino acid sequence. The difference in sequence would make homology-based gene identification strategies, like EST libraries, less effective.

7. CONCLUSION

There are still many unanswered questions regarding the terpenoid biosynthesis within the biseriate glandular trichomes of *A. annua*. Although we do not know the full story behind trichome specific gene expression and terpenoid metabolism, there are some points that we have addressed in this study.

We now have a proven method for the isolation of glandular trichomes from *A. annua*. This technique is most suited to floral tissue which is easy to generate and stage by adjusting the photoperiod in which the plants are grown. RT-PCR expression profiles which confirmed trichome specificity for AaMTADH, AMDS, AaALDH, and CYP71AV1 were generated. For the first time, a gene was localized using WISH to a specific cell pair(s) within a biseriate trichome. This will allow us to better understand the possible biosynthetic specialization in the glandular trichomes of *A. annua* and related species. The WISH results also suggest that the AMDS promoter that was isolated can be used to drive trichome-specific gene expression. Finally, we have identified a new monoterpene dehydrogenase, AaMTADH. It shows a trichome specific expression pattern. It has broad substrate range, catalyzing the oxidation of most of the secondary monoterpene alcohols found in the essential oil including borneol, artemisia alcohol, pinocarveol, and fenchol. It does not appear to have any role in the biosynthesis of the sesquiterpene lactone artemisinin. It belongs to the short chain alcohol dehydrogenase family with an open reading frame of 798 nucleotides and produces an active protein of ~28126 daltons. The pH optimum of AaMTADH utilizing artemisia alcohol as a substrate is 10.0.

8. FUTURE RESEARCH

This study focused on the isolation of trichomes for the purpose of studying trichome-specific gene expression. The cell-specific gene expression of AMDS within the glandular trichomes was achieved using WISH and a novel enzyme AaMTADH was isolated and partially characterized. However, this has only scratched the surface of the complexity of the glandular trichomes of *A. annua*. Other enzymes involved the artemisinin biosynthesis pathway such as AaALDH1 and CYP71AV1 should be localized within the trichome. Although it was unsuccessful in this study, traditional *in situ* hybridization would probably be the most successful technique to use for that investigation. However, it would require a significant investment of time and expertise to be successful. Genes in other pathways could also be investigated such as other mono and sesqui-terpene synthases and AaMTADH. The results of these localizations could determine whether or not there is any biochemical specialization of cell pairs within the *A. annua* glandular trichome. Furthermore, it would also be useful to show subcellular localization of the various enzymes involved in mono and sesqui-terpene biosynthesis. This would give an in-depth look at the possibility of metabolic channeling (Jorgensen *et al.*, 2005) and could be compared to the localization of the transcripts to investigate whether any proteins are transported within the trichome or cuticular sac (Sirikantaramas *et al.*, 2005).

The amorpha-4,11-diene synthase promoter sequence specificity and induction conditions could be investigated in a system such as *Helianthus annuus* (sunflower). Although it has more cell pairs within the trichomes (18-22 cell pairs), they retain the basic structure of *A. annua* possessing a biseriate morphology (Gopfert *et al.*, 2005). However, the trichomes of *Helianthus annuus* appear to have three non-green apical cell pairs on top of possibly 5 or 6 green cell pairs. Whether any cell pair expression that the AMDS promoter may exhibit in *A. annua* would be reproduced in any useful manner is uncertain. Other parameters, such as stimuli testing would presumably be possible and should have relevance to *A. annua*.

The isolation, pH optimum determination, and substrate testing of AaMTADH formed a foundation upon which more characterization can be performed. The enzyme needs to be fully characterized kinetically using the substates which were shown in this study to be

utilized by AaMTADH. The results of that analysis will give insight as to which monoterpenol is preferred by the enzyme in the trichome. Localization of the enzyme within the trichome could give more information about where and when the monoterpenols are converted to their ketone form. This may be important if there is any usefulness of the ketone form over the alcohol form for either natural or commercial purposes.

9. REFERENCES

Abdin, M.Z., Israr, M., Rehman, R.U., and Jain, S.K. (2003). Artemisinin, a novel antimalarial drug: biochemical and molecular approaches for enhanced production. Planta Med. *69*, 289-299.

Akers, C.P., Weybrew, J.A., and Long, R.C. (1978). Ultrastructure of glandular trichomes of leaves of *Nicotiana tabacum* L., cv Xanthi. Amer. J. Bot. *65*, 282-292.

Bach, T.J. (1995). Some new aspects of isoprenoid biosynthesis in plants--a review. Lipids *30*, 191-202.

Banerjee, S., Zehra, M., Gupta, M.M., and Kumar, S. (1997). *Agrobacterium rhizogenes*-mediated transformation of *Artemisia annua*: production of transgenic plants. Planta Med. *63*, 467-469.

Bertea, C.M., Freije, J.R., van der Woude, H., Verstappen, F.W., Perk, L., Marquez, V., de Kraker, J.W., Posthumus, M.A., Jansen, B.J., de Groot, A., *et al.* (2005). Identification of intermediates and enzymes involved in the early steps of artemisinin biosynthesis in *Artemisia annua* Planta Med. *71*, 40-47.

Bhakuni, R.S., Jain, D.C., Sharma, R.P., and Kumar, S. (2001). Secondary metabolites of *Artemisia annua* and their biological actiivity. Curr. Sci. *80*, 35-48.

Bloch, K. (1992). Sterol molecule: structure, biosynthesis, and function. Steroids *57*, 378-383.

Bohlmann, J., Meyer-Gauen, G., and Croteau, R. (1998). Plant terpenoid synthases: molecular biology and phylogenetic analysis. Proc. Natl. Acad. Sci. U.S.A. *95*, 4126-4133.

Bouwmeester, H.J., Wallaart, T.E., Janssen, M.H., van Loo, B., Jansen, B.J., Posthumus, M.A., Schmidt, C.O., de Kraker, J.W., Konig, W.A., and Franssen, M.C. (1999). Amorpha-4,11-diene synthase catalyses the first probable step in artemisinin biosynthesis. Phytochemistry *52*, 843-854.

Brown, G.D., and Sy, L.K. (2004). In vivo transformations of dihydroartemisinic acid in *Artemisia annua* plants. Tetrahedron *60*, 1139-1159.

Brown, G.D., and Sy, L.K. (2007). In vivo transformations of dihydro-epi-deoxyarteannuin B in *Artemisia annua* plants. Tetrahedron *63*, 9536-9547.

Cano Abad, M., Di Benedetto, G., Magalhaes, P., Filippin, L., and Pozzan, T. (2004). Mitochondrial pH monitored by a new engineered green fluorescent protein mutant. J. Biol. Chem. *279*, 11521-11529

Chang, M.C.Y., and Keasling, J.D. (2006). Production of isoprenoid pharmaceuticals by engineered microbes. Nat. Chem. Biol. *2*, 674-681.

Charles, D.J., Cebert, E., and Simon, J.E. (1991). Characterization of the essential oil of *Artemisia annua* L. J. Essent. Oil Res. *3* 33-39.

Chen, D., Liu, C., Ye, H., Li, G., Liu, B., Meng, Y., and Chen, X. (1999). Ri-mediated transformation of *Artemisia annua* with a recombinant farnesyl diphosphate synthase gene for artemisinin production Plant. Cell. Tiss. Org. *57*, 157-162.

Chen, D., Ye, H., and Li, G. (2000). Expression of a chimeric farnesyl diphosphate synthase gene in *Artemisia annua* L. transgenic plants via *Agrobacterium tumefaciens*-mediated transformation. Plant Sci. *155*, 179-185.

Covello, P.S., Teoh, K.H., Polichuk, D.R., Reed, D.R., and Nowak, G. (2007). Functional genomics and the biosynthesis of artemisinin. Phytochemistry *68*, 1864-1871.

Cox, K.H., Goldberg, R.B., and Shaw, C.H. (1988). Analysis of Plant Gene Expression. In Plant Molecular Biology: A practical approach (Oxford: IRL Press), pp. 1-34.

Croteau, R. (1977). Site of monoterpene biosynthesis in *Majorana hortensis* leaves. Plant Physiol. *59*, 519-520.

Croteau, R., Felton, M., Karp, F., and Kjonaas, R. (1981). Relationship of camphor biosynthesis to leaf development in sage (*Salvia officinalis*). Plant Physiol. *67*, 820-824.

Croteau, R., and Karp, F. (1979). Biosynthesis of monoterpenes: hydrolysis of bornyl pyrophosphate, an essential step in camphor biosynthesis, and hydrolysis of geranyl pyrophosphate, the acyclic precursor of camphor, by enzymes from sage (*Salvia officinalis*). Arch. Biochem. Biophys. *198*, 523-532.

Croteau, R.B., Davis, E.M., Ringer, K.L., and Wildung, M.R. (2005). Menthol biosynthesis and molecular genetics. Naturwissenschaften *92*, 562-577.

Davidson, T.A., Mondal, K., and Yang, X. (2004). Use of a chiral surfactant for enantioselective reducation of a ketone. J. Coll. Interf. Sci. *15*, 498-502.

Dell, B., McComb, J.A. (1978). Plant resins-- their formation, secretion and possible functions. Adv. Bot. Res. *6*, 276-316.

Dewick, P.M. (2002). Medicinal natural products:A biosynthetic approach, 2 edn (Chichester, UK: Wiley).

Dubey, V.S., Bhalla, R., and Luthra, R. (2003). An overview of the non-mevalonate pathway for terpenoid biosynthesis in plants. J. Biosciences *28*, 637-646.

Duke, M.V., Paul, R.N., Elsohly, H.N., Sturtz, G., and Duke, S.O. (1994). Localization of artemisinin and artemisitene in the foliar tissues of glanded and glandless biotypes of *Artemisia annua* L. Int. J. Plant Sci. *155* 365-372.

Duke, S.O., and Paul, R.N. (1993). Development and fine structure of glandular trichomes of *Artemisia annua* L. Int. J. Plant. Sci. *154*, 107-118.

Efferth, T. (2006). Molecular pharmacology and pharmacogenomics of artemisinin and its derivatives in cancer cells. Curr. Drug Targets *7*, 407-421.

Eisenreich, W., Schwarz, M., Cartayrade, A., Arigoni, D., Zenk, M.H., and Bacher, A. (1998). The deoxyxylulose phosphate pathway of terpenoid biosynthesis in plants and microorganisms. Chem. Biol. *5*, R221-233.

Engler, J.A., Montagu, M.V., Engler, G., Martinez-Zapater, J.M., and Salinas, J. (1998). Whole-Mount *In Situ* Hybridization in Plants. In Arabidopsis Protocols, J.M. Walker, ed. (Totowa, NJ: Humana Press), pp. 373-384.

Fahn, A. (1988). Secretory tissue in plants. New Phytol. *108*, 229-257.

Ferreira, J.F., Simon, J.E., and Janick, J. (1995). Developmental studies of *Artemisia annua*: flowering and artemisinin production under greenhouse and field conditions. Planta Med. *61*, 167-170.

Ferreira, J.F., Simon, J.E., and Janick, J. (1997). *Artemisia Annua*: botany, horticulture, pharmacology. In Horticultural reviews, J. Janick, ed. (New York, NY: John Wiley & Sons, Inc.), pp. 319-371.

Ferreira, J.F.S., and Janick, J. (1995). Floral morphology of *Artemisia annua* with special reference to trichomes. Int. J. Plant Sci. *156* 807-815.

Ferreira, J.F.S., Janick, J. (1996). Distribution of Artemisinin in *Artemisia Annua* In Progress in new crops (Arlington, VA: ASHS Press), pp. 579-584.

Ferreira, J.F.S., Laughlin, J.C., Delabays, N., and de Magalhaes, P.M. (2005). Cultivation and genetics of *Artemisia annua* L. for the increased production of the antimalarial artemisinin Plant Gen. Resources *3*, 206-229.

Gershenzon, J., and Dudareva, N. (2007). The function of terpene natural products in the natural world. Nat. Chem. Biol. *3*, 408-414.

Gershenzon, J., McKaskill, D., Rajaonarivony, J.I.M., Mihaliak, C., Karp, F., and Croteau, R. (1992). Isolation of secretory cells from plant glandular trichomes and their use in biosynthetic studies of monoterpenes and other gland products. Anal. Biochem. *200*, 130-138.

Ghosh, B., Mukherjee, S., and Jha, S. (1997). Genetic transformation of *Artemisia annua* by *Agrobacterium tumefaciens* and artemisinin synthesis in transformed cultures Plant Sci. *122*, 193-199.

Gopfert, J.C., Heil, N., Conrad, J., and Spring, O. (2005). Cytological development and sesquiterpene lactone secretion in capitate glandular trichomes of sunflower. Plant Biol. *7*, 148-155.

Hall, H.M., Clements, F.E. (1932). The North American species of Artemisia, Chrysothamnus and Atriplex In The Phylogenetic Method in Taxonomy (Washington, WA: Carnegie Inst.), pp. 310-311.

Han, J., Wang, H., Ye, H., Liu, Y., Li, Z., Zhang, Y., Zhang, Y., Yan, F., and Li, G. (2005). High efficiency of genetic transformation and regeneration of *Artemisia annua* L. via *Agrobacterium tumefaciens*-mediated procedure. Plant Sci. *168*, 73-80.

Harrewijn, P., van Oosten, A.M., and Piron, P.G.M. (2001). Natural terpenoids as messengers: A multidisciplinary study of their production, biological functions and practical applications (Boston, MA: Kluwer Academic Publishers).

He, X.C., Zeng, M.Y., Li, G.F., and Liang, Z. (1983). Callus induction and regeneration of plantlets from *Artemisia annua* and changes of qinghaosu contents. Acta Bot. Sin. *25*, 87–90.

Hsu, E. (2006). The history of qing hao in the Chinese materia medica. T. Roy. Soc. Trop. Med. H. *100*, 505-508.

Hulskamp, M., Misra, S., and Jurgens, G. (1994). Genetic dissection of trichome cell development in Arabidopsis. Cell *76*, 555-566.

Hunter, W.N. (2007). The non-mevalonate pathway of isoprenoid precursor biosynthesis. J. Biol. Chem. *282*, 21573-21577.

Iijima, Y., Davidovich-Rikanati, R., Fridman, E., Gang, D.R., Bar, E., Lewinsohn, E., and Pichersky, E. (2004). The biochemical and molecular basis for the divergent patterns in the biosynthesis of terpenes and phenylpropenes in the peltate glands of three cultivars of basil. Plant Physiol. *136*, 3724-3736.

Jaziri, M., Shimomura, K., Yoshimatsu, K., Fauconnier, M.L., Marlier, M., and Homes, J. (1995). Establisment of normal and transformed root cultures of *Artemisia annua* L. for artemisinin produciton. J. Plant. Physiol. *145*, 175-177.

Jefford, C.W. (2007). New developments in synthetic peroxidic drugs as artemisinin mimics. Drug Discov. Today *12*, 487-495.

Johnson, H.B. (1975). Plant pubescence: An ecological perspective. Bot. Rev. *41*, 233-258.

Jorgensen, K., Rasmussen, A.V., Morant, M., Nielsen, A.H., Bjarnholt, N., Zagrobelny, M., Bak, S., and Moller, B.L. (2005). Metabolon formation and metabolic channeling in the biosynthesis of plant natural products. Curr. Opin. Plant Biol. *8*, 280-291.

Jung, M., Lee, K., Kim, H., and Park, M. (2004). Recent advances in artemisinin and its derivatives as antimalarial and antitumor agents. Curr. Med. Chem. *11*, 1265-1284.

Kaiser, A., Gottwald, A., Wiersch, C., Maier, W., and Seitz, H.M. (2002). The necessity to develop drugs against parasitic diseases. Pharmazie *57*, 723-728.

Klayman, D.L. (1985). Qinghaosu (artemisinin): an antimalarial drug from China. Science *228*, 1049-1055.

Klayman, D.L. (1989). Weeding out malaria. Nat. Hist. *3*, 18-26.

Klayman, D.L. (1993). *Artemisia annua*: From weed to respectable antimalarial plant. In Human Medicinal Agents from Plants, A.D. Kinghorn, and M.F. Balandrin, eds. (Washington, DC), pp. 242-255.

Krozowski, Z. (1994). The short-chain alcohol dehydrogenase superfamily: variations on a common theme. J. Steroid Biochem. *51*, 125-130.

Kumar, M., and Ando, Y. (2006). Carbon nanotubes from camphor: an environment-friendly nanotechnology. J. Phys. : Conf. Ser. *61*, 643-646.

Lange, B.M., and Croteau, R. (1999). Genetic engineering of essential oil production in mint. Curr. Opin. Plant Biol. *2*, 139-144.

Lange, B.M., Wildung, M.R., Stauber, E.J., Sanchez, C., Pouchnik, D., and Croteau, R. (2000). Probing essential oil biosynthesis and secretion by functional evaluation of expressed sequence tags from mint glandular trichomes. Proc. Natl. Acad. Sci. U.S.A. *97*, 2934-2939.

Lee, S. (2007). Artemisinin, promising lead natural product for various drug developments. Mini Rev. Med. Chem. *7*, 411-422.

Lessire, R., Abdulkarim, T., and Cassagne, C. (1982). Origin of the wax of very long chain fatty acids in leek, *Allium porrum* L., leaves: a plausible model. In The Plant Cuticle, K.L. Cutler, D.F. Alvin, and C.E. Price, eds. (London, UK: Academic Press), pp. 167-180.

Levin, D.V. (1973). The role of trichomes in plant defense. Q. Rev. Biol. *48*, 3-15.

Li, J., and Chory, J. (1998). Preparation of DNA from Arabidopsis In Methods in Molecular Biology, J. Martinez-Zapater, and J. Salinas, eds. (Totowa, NJ: Humana Press), pp. 55-60.

Li, Y., Huang, H., and Wu, Y.L. (2006). Qinghaosu artemisinin - a fantastic antimalarial drug from a traditional Chinese medicine. In Medicinal Chemistry of Bioactive Natural Products, X.T. Liang, and W.S. Fang, eds. (New York, NY: John Wiley & Sons, Inc.), pp. 183-256.

Liu, C. (2003). Factors influencing artemisinin production from shoot cultures of *Artemisia annua* L. World J. Microb. Biot. *19*, 535-538.

Liu, C., Guo, C., Wang, Y., and Ouyang, F. (2004). Factors influencing artemisinin production from shoot cultures of *Artemisia annua* L. World J. Microb. Biot. *19*, 535-538.

Liu, C.Z., Wang, Y.C., Ouyang, F., Ye, H.C., and Li, G.F. (1997). Production of artemisinin by hairy root cultures of *Artermisia annua* L. Biotechnol. Lett. *19*, 927-930.

Liu, J.M., Ni, M.Y., Fan, J.F., Tu, Y.Y., Wu, Z.H., Wu, Y.L., and Chou, W.S. (1979). Structure and reaction of arteannuin. Acta Chim. Sin. *37*, 129-143.

Logemann, J., Schell, J., and Willmitzer, L. (1987). Improved method for the isolation of RNA from plant tissues. Anal. Biochem. *163*, 16-20.

Loza-Tavera, H. (1999). Monoterpenes in essential oils. Biosynthesis and properties. Adv. Exp. Med. Biol. *464*, 49-62.

Lupien, S., Karp, F., Ponnamperuma, K., Wildung, M., and Croteau, R. (1995). Cytochrome P450 limonene hydroxylases of Mentha species. Drug Metabol. Drug Interact. *12*, 245-260.

Maffei, M., and Sacco, T. (1987). Chemical and morphometrical comparison between two Peppermint notomorphs. Planta Med. *53*, 214-216.

Mano, J., Belles-Boix, E., Babiychuk, E., Inze, D., Torii, Y., Hiraoka, E., Takimoto, K., Slooten, L., Asada, K., and Kushnir, S. (2005). Protection against photooxidative injury of tobacco leaves by 2-alkenal reductase: detoxification of lipid peroxide-derived reactive carbonyls. Plant Physiol. *139*, 1773-1783.

Marks, M.D. (1997). Molecular genetic analysis of trichome development in Arabidopsis. Annu. Rev. Plant Physiol. Plant Mol. Biol. *48*, 137-163.

McKay, D.L., and Blumberg, J.B. (2006). A review of the bioactivity and potential health benefits of peppermint tea (*Mentha piperita* L.). Phytother. Res. *20*, 619-633.

McVaugh, R., ed. (1984). Compositae (Ann Arbor, MI: University of Michigan Press).

Nair, M.S., Acton, N., Klayman, D.L., Kendrick, K., Basile, D.V., and Mante, S. (1986). Production of artemisinin in tissue cultures of *Artemisia annua*. J. Nat. Prod. *49*, 504-507.

Nakase, I., Lai, H., Singh, N.P., and Sasaki, T. (2007). Anticancer properties of artemisinin derivatives and their targeted delivery by transferrin conjugation. Int. J. Pharm.

O'Neill, P.M. (2005). The therapeutic potential of semi-synthetic artemisinin and synthetic endoperoxide antimalarial agents. Expert Opin. Investig. Drugs *14*, 1117-1128.

Paeshuyse, J., Coelmont, L., Vliegen, I., Van hemel, J., Vandenkerckhove, J., Peys, E., Sas, B., De Clercq, E., and Neyts, J. (2006). Hemin potentiates the anti-hepatitis C virus activity of the antimalarial drug artemisinin. Biochem. Biophys. Res. Commun. *348*, 139-144.

Qian, Z., Gong, K., Zhang, L., Lv, J., Jing, F., Wang, Y., Guan, S., Wang, G., and Tang, K. (2007). A simple and efficient procedure to enhance artemisinin content in *Artemisia annua* L. by seeding to salinity stress Afr. J. Biotech. *6*, 1410-1413.

Reed, D.W., Polichuk, D.R., Buist, P.H., Ambrose, S.J., Sasata, R.J., Savile, C.K., Ross, A.R., and Covello, P.S. (2003). Mechanistic study of an improbable reaction: alkene dehydrogenation by the delta12 acetylenase of *Crepis alpina*. J. Am. Chem. Soc. *125*, 10635-10640.

Ringer, K.L., Davis, E.M., and Croteau, R. (2005). Monoterpene metabolism. cloning, expression, and characterization of (-)-isopiperitenol/(-)-carveol dehydrogenase of Peppermint and Spearmint. Plant Physiol. *137*, 863-872.

Ro, D.K., Paradise, E.M., Ouellet, M., Fisher, K.J., Newman, K.L., Ndungu, J.M., Ho, K.A., Eachus, R.A., Ham, T.S., Kirby, J.*, et al.* (2006). Production of the antimalarial drug precursor artemisinic acid in engineered yeast. Nature *440*, 940-943.

Rohmer, M. (1998). Isoprenoid biosynthesis via the mevalonate-independent route, a novel target for antibacterial drugs? Prog. Drug. Res. *50*, 135-154.

Romero, M.R., Efferth, T., Serrano, M.A., Castano, B., Macias, R.I., Briz, O., and Marin, J.J. (2005). Effect of artemisinin/artesunate as inhibitors of hepatitis B virus production in an "*in vitro*" replicative system. Antiviral Res. *68*, 75-83.

Sacchettini, J.C., and Poulter, C.D. (1997). Creating isoprenoid diversity. Science *277*, 1788-1789.

Sarker, G., Turner, R.T., and Bolander, M.E. (1993). Restriction-site PCR: a direct method of unknown sequence retrieval adjacent to a known locus by using universal primers. PCR Meth. Appl. *2*, 318-322.

Schilmiller, A.L., Last, R.L., and Pichersky, E. (2008). Harnessing plant trichome biochemistry for the production of useful compounds. Plant J. *54*, 702-711.

Schoonhoven, L.M., van Loon, J.J.A., and Dicke, M. (2005). Insect-plant Biology: from physiology to evolution (New York, NY: Oxford University Press).

Schutz, K., Carle, R., and Schieber, A. (2006). Taraxacum-a review on its phytochemical and pharmacological profile. J. Ethnopharmacol. *107*, 313-323.

Schwab, B., Folkers, U., Ilgenfritz, H., and Hulskamp, M. (2000). Trichome morphogenesis in Arabidopsis. Philos. Trans. R. Soc. Lond. B. Biol. Sci. *355*, 879-883.

Seigler, D.S. (1995). Plant Secondary Metabolism (Boston, MA: Kluwer Academic Publishers).

Sirikantaramas, S., Taura, F., Tanaka, Y., Ishikawa, Y., Morimoto, S., and Shoyama, Y. (2005). Tetrahydrocannabinolic acid synthase, the enzyme controlling marijuana psychoactivity, is secreted into the storage cavity of the glandular trichomes. Plant Cell Physiol. *46*, 1578-1582.

Slone, J.H., and Kelsey, R.G. (1985). Isolation and purification of glandular secretory cells from *Artemisia Tridentata* (SSP. Vaseyana) by percoll density gradient centrifugation. Amer. J. Bot. *72*, 1445-1451.

Stephenson, I., and Wiselka, M. (2000). Drug treatment of tropical parasitic infections: recent achievements and developments. Drugs *60*, 985-995.

Swanson, K.M., and Hohl, R.J. (2006). Anti-cancer therapy: targeting the mevalonate pathway. Curr. Cancer Drug Targets *6*, 15-37.

Sy, L.K., and Brown, G.D. (2002). The mechanism of the spontaneous autoxidation of dihydroartemisinic acid. Tetrahedron *58*, 897-908.

Tawfig, N.K., Anderzon, L.A., Roberts, M.F., Philipson, J.D., Bray, D.H., and Warhurst, D.C. (1989). Antiplasmodial activity of *Artemisia annua* plant cell culture. Plant Cell Rep. *8*, 425-428.

Teixeira da Silva, J.A. (2004). Mining the essential oil of the Anthemideae. Afr. J. Biotechnol. *3*, 706-720.

Teoh, K.H., Polichuk, D.R., Reed, D.W., Nowak, G., and Covello, P.S. (2006). *Artemisia annua* L. (Asteraceae) trichome-specific cDNAs reveal CYP71AV1, a cytochrome P450 with a key role in the biosynthesis of the antimalarial sesquiterpene lactone artemisinin. FEBS Lett. *580*, 1411-1416.

Turner, G.W., and Croteau, R. (2004). Organization of monoterpene biosynthesis in Mentha. Immunocytochemical localizations of geranyl diphosphate synthase, limonene-6-hydroxylase, isopiperitenol dehydrogenase, and pulegone reductase. Plant Physiol. *136*, 4215-4227.

Turner, G.W., Gershenzon, J., and Croteau, R.B. (2000a). Development of peltate glandular trichomes of peppermint. Plant Physiol. *124*, 665-680.

Turner, G.W., Gershenzon, J., and Croteau, R.B. (2000b). Distribution of peltate glandular trichomes on developing leaves of peppermint. Plant Physiol. *124*, 655-664.

Umlauf, D., Zapp, J., Becker, H., and Adam, K.P. (2004). Biosynthesis of the irregular monoterpene artemisia ketone, the sesquiterpene germacrene D and other isoprenoids in *Tanacetum vulgare* L. (Asteraceae). Phytochemistry *65*, 2463-2470.

van der Werf, M., van der Ven, C., Barbirato, F., Eppink, M., de Bont, J., and van Berkel, W. (1999). Stereoselective carveol dehydrogenase from *Rhodococcus erythropolis* DCL14. J. Biol. Chem. *274*, 26296-26304.

Venkatachalam, K.V., Kjonaas, R., and Croteau, R. (1984). Development and essential oil content of secretory glands of sage (*Salvia officinalis*). Plant Physiol. *76*, 148-150.

Vergauwe, A., Van Geldre, E., Inzé, D., Van Montagu, M., and Van den Eeckhout, E. (1997). Factors influencing *Agrobacterium tumefaciens*-mediated transformation of *Artemisia annua* L. . Plant Cell Rep. *18*, 105-110.

Wagner, G.J. (1991). Secreting glandular trichomes: more than just hairs. Plant Physiol. *96*, 675-679.

Wagner, G.J., Wang, E., and Shepherd, R.W. (2004). New approaches for studying and exploiting an old protuberance, the plant trichome. Ann. Bot. *93*, 3-11.

Wang, E., Wang, R., DeParasis, J., Loughrin, J.H., Gan, S., and Wagner, G.J. (2001a). Suppression of a P450 hydroxylase gene in plant trichome glands enhances natural-product-based aphid resistance. Nat. Biotechnol. *19*, 371-374.

Wang, J.W., and Tan, R.X. (2002). Artemisinin production in *Artemisia annua* hairy root cultures with improved growth by altering the nitrogen source in the medium Biotechnol. Lett. *24*, 1153-1156.

Wang, J.W., Zhang, Z., and Tan, R.X. (2001b). Stimulation of artemisinin production in *Artemisia annua* hairy roots by the elicitor from the endophytic Colletotrichum sp. . Biotechnol. Lett. *23*, 857-860.

Weathers, P.J., Cheethan, R.D., Follansbee, E., and Theohairides, K. (1994). Artemisinin production by transformed roots of *Artemisia annua*. Biotechnol. Lett. *16*, 1281-1286.

Weathers, P.J., DeJesus-Gonzalez, L., Kim, Y.J., Souret, F.F., and Towler, M.J. (2004). Alteration of biomass and artemisinin production in *Artemisia annua* hairy roots by media sterilization method and sugars. Plant Cell Rep. *23*, 414-418.

Withers, S.T., and Keasling, J.D. (2007). Biosynthesis and engineering of isoprenoid small molecules. Appl. Microbiol. Biotechnol. *73*, 980-990.

Woerdenbag, H.J., Luers, J.F.J., Van Uden, W., Pras, N., Malingre, T.H., and Alfermann, A.W. (1993). Production of the new antimalarial drug artemisinin in shoot cultures of *Artemisia annua* L. Plant Cell Tiss. Org. *32*, 247–257.

Worthington, C. (1993). Alcohol Dehydrogenase. In Worthington Enzyme Manual, W.B. Corporation, ed. (Freehold, NJ: Worthington Biochemical Corporation).

Yamaura, T., Tanaka, S., and Tabata, M. (1992). Localization of the biosynthesis and accumulation of monoterpenoids in glandular trichomes of thyme. Planta Med. *58*, 153-158.

Yerger, E.H., Grazzini, R.A., Hesk, D., Cox-Foster, D.L., Craig, R., and Mumma, R.O. (1992). A rapid method for isolating glandular trichomes. Plant Physiol. *99*, 1-7.

Zhang, X., and Oppenheimer, D.G. (2004). A simple and efficient method for isolating trichomes for downstream analyses. Plant Cell Physiol. *45*, 221-224.

Ziegler, J., Voigtlander, S., Schmidt, J., Kramell, R., Miersch, O., Ammer, C., Gesell, A., and Kutchan, T.M. (2006). Comparative transcript and alkaloid profiling in Papaver species identifies a short chain dehydrogenase/reductase involved in morphine biosynthesis. Plant J. *48*, 177-192.